

TRAINING COURSE IN GEOTECHNICAL AND FOUNDATION ENGINEERING

NHI COURSE NO. 13239 - MODULE 9

PUBLICATION NO. FHWA HI-99-012
DECEMBER 1998

GEOTECHNICAL EARTHQUAKE ENGINEERING

REFERENCE MANUAL



U.S. Department
of Transportation

**Federal Highway
Administration**



National Highway Institute

Technical Report Documentation Page

1. Report No. FHWA-HI-99-012		2. Government Accession No.		3. Recipient's Catalog No.	
4. Title and Subtitle GEOTECHNICAL EARTHQUAKE ENGINEERING REFERENCE MANUAL				5. Report Date December 1998	
				6. Performing Organization Code	
7. Author(s) Principal Investigator: George Munfakh* Authors: Edward Kavazanjian, Jr.▲, Neven Matasović▲, Tarik Hadj-Hamou▲, and Jaw-Nan (Joe) Wang*				8. Performing Organization Report No.	
9. Performing Organization Name and Address * Parsons Brinckerhoff Quade & Douglas, Inc. One Penn Plaza, New York, NY 10119 In association with: ▲ GeoSyntec Consultants 2100 Main St., Suite 150, Huntington Beach, CA 92648				10. Work Unit No. (TRAI5)	
				11. Contract or Grant No. DTFH61-94-C-00104	
12. Sponsoring Agency Name and Address Federal Highway Administration National Highway Institute 901 North Stuart Street, Suite 300 Arlington, Virginia 22203				13. Type of Report and Period Covered	
				14. Sponsoring Agency Code	
15. Supplementary Notes FHWA Technical Consultants - J.A. DiMaggio, A. Munoz and P. Osborn FHWA Contracting Officer - J. Mowery III; COTR - L. Jones, National Highway Institute					
16. Abstract This manual has been written to provide training on how to apply principles of geotechnical earthquake engineering to planning, design, and retrofit of highway facilities. Geotechnical earthquake engineering topics discussed in Part I of this manual include: <ul style="list-style-type: none"> • deterministic and probabilistic seismic hazard assessment; • evaluation of design ground motions; • seismic site response analyses; • evaluation of liquefaction potential and seismic settlements; • seismic slope stability and deformation analyses; and • seismic design of foundations and retaining structures. The manual provides detailed information on basic principles and analyses, with reference to where detailed information on these analyses can be obtained. Design examples illustrating these principles and analyses are provided in Part II of this manual.					
17. Key Words Geotechnical earthquake engineering, soil dynamics, engineering seismology, engineering geology, liquefaction, slopes, foundations, retaining walls			18. Distribution Statement No restrictions.		
19. Security Classif. (of this report) UNCLASSIFIED		20. Security Classif. (of this page) UNCLASSIFIED		21. No. of Pages 392	22. Price

MODULE 9

TABLE OF CONTENTS

PART I- DESIGN PRINCIPLES

	Page
LIST OF FIGURES	viii
LIST OF TABLES	xii
LIST OF SYMBOLS	xiii
1.0 Introduction	1-1
1.1 Introduction	1-1
1.2 Sources of Damage in Earthquakes	1-2
1.2.1 General	1-2
1.2.2 Direct Damage	1-2
Classification of Direct Damage	1-2
Primary Damage	1-2
Secondary Damage	1-3
1.2.3 Indirect Damage	1-5
1.3 Earthquake-Induced Damage to Highway Facilities	1-6
1.3.1 Overview	1-6
1.3.2 Historical Damage to Highway Facilities	1-6
1.4 Organization of the Document	1-8
2.0 Earthquake Fundamentals	2-1
2.1 Introduction	2-1
2.2 Basic Concepts	2-1
2.2.1 General	2-1
2.2.2 Plate Tectonics	2-1
2.2.3 Fault Movements	2-3
2.3 Definitions	2-6
2.3.1 Introduction	2-6
2.3.2 Type of Faults	2-6
Strike Slip Faults	2-6
Dip Slip Faults	2-6
Other Special Cases	2-6
2.3.3 Earthquake Magnitude	2-7
2.3.4 Hypocenter and Epicenter	2-8
2.3.5 Zone of Energy Release	2-8
2.3.6 Site-to-Source Distance	2-9
2.3.7 Peak Ground Motions	2-9
2.3.8 Response Spectrum	2-12
2.3.9 Attenuation Relationships	2-14
2.3.10 Intensity Scales	2-14

3.0	Seismic Hazard Analysis	3-1
3.1	General	3-1
3.2	Seismic Source Characterization	3-1
3.2.1	Overview	3-1
3.2.2	Methods for Seismic Source Characterization	3-2
3.2.3	Defining the Potential for Fault Movement	3-4
3.2.4	Seismic Source Characterization in the Eastern and Central States	3-5
3.3	The Determination of the Intensity of Design Ground Motions	3-6
3.3.1	Introduction	3-6
3.3.2	Published Codes and Standards	3-6
3.3.3	The Deterministic Approach	3-14
3.3.4	The Probabilistic Approach	3-15
4.0	Ground Motion Characterization	4-1
4.1	Basic Ground Motion Characteristics	4-1
4.2	Peak Values	4-1
4.2.1	Evaluation of Peak Parameters	4-1
4.2.2	Attenuation of Peak Values	4-2
4.2.3	Selection of Attenuation Relationships	4-4
4.2.4	Selection of Attenuation Relationship Input Parameters	4-8
4.2.5	Distribution of Output Ground Motion Parameter Values	4-8
4.3	Frequency Content	4-9
4.4	Energy Content	4-11
4.5	Duration	4-13
4.6	Influence of Local Site Conditions	4-16
4.6.1	Local Site Effect	4-16
4.6.2	Codes and Standards	4-18
4.6.3	Energy and Duration	4-24
4.6.4	Resonant Site Frequency	4-24
4.7	Selection of Representative Time Histories	4-26
5.0	Site Characterization	5-1
5.1	Introduction	5-1
5.2	Subsurface Profile Development	5-1
5.2.1	General	5-1
5.2.2	Water Level	5-1
5.2.3	Soil Stratigraphy	5-2
5.2.4	Depth to Bedrock	5-3
5.3	Required Soil Parameters	5-3
5.3.1	General	5-3
5.3.2	Relative Density	5-3
5.3.3	Shear Wave Velocity	5-4
5.3.4	Cyclic Stress-Strain Behavior	5-5
5.3.5	Peak and Residual Shear Strength	5-7
5.4	Evaluation of Soil Properties	5-8
5.4.1	General	5-8
5.4.2	In Situ Testing for Soil Profiling	5-9
	Standard Penetration Testing (SPT)	5-9
	Cone Penetration Testing (CPT)	5-14

5.4.3	Soil Density	5-15
5.4.4	Shear Wave Velocity	5-15
	General	5-15
	Geophysical Surveys	5-15
	Compressional Wave Velocity	5-22
5.4.5	Evaluation of Cyclic Stress-Strain Parameters	5-22
	Laboratory Testing	5-22
	Use of Empirical Correlations	5-23
5.4.6	Peak and Residual Shear Strength	5-26
6.0	Seismic Site Response Analysis	6-1
6.1	General	6-1
6.2	Site-Specific Site Response Analysis	6-1
6.3	Simplified Seismic Site Response Analyses	6-1
6.4	Equivalent-Linear One-Dimensional Site Response Analyses	6-6
6.5	Advanced One- and Two-Dimensional Site Response Analyses	6-9
	6.5.1 General	6-9
	6.5.2 One-Dimensional Non-Linear Response Analyses	6-9
	6.5.3 Two-Dimensional Site Response Analyses	6-10
7.0	Seismic Slope Stability	7-1
7.1	Background	7-1
7.2	Seismic Coefficient-Factor of Safety Analyses	7-3
	7.2.1 General	7-3
	7.2.2 Selection of the Seismic Coefficient	7-4
7.3	Permanent Seismic Deformation Analyses	7-6
	7.3.1 Newmark Sliding Block Analysis	7-6
7.4	Unified Methodology for Seismic Stability and Deformation Analysis	7-11
7.5	Additional Considerations	7-13
8.0	Liquefaction and Seismic Settlement	8-1
8.1	Introduction	8-1
8-2	Factors Affecting Liquefaction Susceptibility	8-1
8-3	Evaluation of Liquefaction Potential	8-5
	8.3.1 Introduction	8-5
	8.3.2 Simplified Procedure	8-5
	8.3.3 Variations on the Simplified Procedure	8-12
8-4	Post-Liquefaction Deformation and Stability	8-12
8-5	Seismic Settlement Evaluation	8-17
8-6	Liquefaction Mitigation	8-20
9.0	Seismic Design of Foundations and Retaining Walls	9-1
9.1	Introduction	9-1
	9.1.1 Seismic Response of Foundation Systems	9-1
	9.1.2 Seismic Performance of Retaining Walls	9-3
9.2	Design of Shallow Foundations	9-3
	9.2.1 General	9-3
	9.2.2 Pseudo-Static Analyses	9-5
	General	9-5
	Load Evaluation for Pseudo-Static Bearing Capacity Analysis	9-5

	The General Bearing Capacity Equation	9-6
	Bearing Capacity from Penetration Tests	9-9
	Sliding Resistance of Shallow Foundations	9-10
	Factors of Safety	9-12
9.2.3	Equivalent Foundation Stiffness	9-12
	General	9-12
	Stiffness Matrix of a Circular Surface Footing	9-13
	Damping	9-14
	Rectangular Footings	9-14
	Embedment Effects	9-16
	Implementation of Dynamic Response Analyses	9-16
9.3	Design of Deep Foundations	9-18
9.3.1	General	9-18
9.3.2	Seismic Vulnerability of Deep Foundations	9-20
9.3.3	General Design Procedure	9-20
9.3.4	Seismic Response of Pile Foundations	9-22
9.3.5	Method of Analysis	9-23
	Group Effects	9-28
9.3.6	Equivalent Foundation Stiffness	9-30
	Equivalent Cantilever Method	9-30
	Foundation Stiffness Matrix Method	9-31
9.3.7	Other Design Issues	9-33
	Foundation Design Forces	9-33
	Soil Strength	9-43
	Pile Uplift Capacity	9-43
	Liquefaction	9-44
	Ground Displacement Loading	9-44
9.4	Retaining Structures	9-45
9.4.1	General	9-45
9.4.2	Gravity Type Retaining Walls	9-46
	Dynamic Earth Pressure Approach	9-46
	Permissible Displacement Approach	9-49
9.4.3	MSE and Soil-Nailed Walls	9-51
	External Seismic Stability	9-52
	Internal Seismic Stability	9-54
9.4.4	Soil-Nailed Walls	9-55
9.4.5	Anchored Walls	9-57
9.4.6	Stiffness of Abutment Walls	9-59
10.0	References	10-1

PART II- DESIGN EXAMPLES

	Page
LIST OF FIGURES	ii
LIST OF TABLES	iv
1.0 Introduction	1-1
2.0 Seismic Analysis of a Shallow Bridge Foundation	2-1
2.1 Introduction	2-1
2.1.1 Description of the Project	2-1
2.1.2 Source Materials Required	2-1
2.2 Site Geology	2-1
2.3 Geotechnical Exploration	2-1
2.4 Design of Shallow Foundation	2-4
2.5 Seismic Settlement and Liquefaction Potential	2-7
2.6 Calculations	2-7
2.7 Summary and Conclusions	2-7
2.8 Detailed Calculations - Example 1 - Seismic Analysis of a Shallow Bridge Foundation	2-7
3.0 Seismic Design of a Deep Foundation System	3-1
3.1 Introduction	3-1
3.1.1 Description of the Project	3-1
3.1.2 Source Materials Required	3-1
3.2 Geotechnical Exploration	3-1
3.3 Design of Pile Foundations	3-5
3.4 Detailed Calculations - Example 2 - Seismic Design of a Deep Foundation System	3-8
3.5 Summary and Conclusion	3-18
4.0 Site Response Analysis	4-1
4.1 Introduction	4-1
4.1.1 Description of the Project	4-1
4.1.2 Source Materials Required	4-1
4.2 Site Conditions	4-1
4.2.1 Subsurface Profile	4-1
4.2.2 Dynamic Soil Properties	4-2
4.2.3 Fundamental Period	4-5
4.3 Seismic Hazard Analysis	4-6
4.3.1 Introduction	4-6
4.3.2 Response Spectra	4-6
4.3.3 Magnitude Distribution	4-6
4.3.4 Selection of Time Histories	4-8
4.4 Seismic Response Analysis	4-9
4.4.1 Method of Analysis	4-9
4.4.2 Results of the Analysis	4-9
5.0 Slope Stability Analysis	5-1

5.1	Introduction	5-1
5.1.1	Description of the Project	5-1
5.1.2	Source Materials Required	5-1
5.2	Site Geology	5-1
5.3	Geotechnical Exploration	5-3
5.3.1	General	5-3
5.3.2	Geotechnical Properties	5-3
5.4	Deterministic Seismic Hazard Analysis	5-3
5.5	Slope Stability Analysis	5-6
5.5.1	Design Criteria	5-6
5.5.2	Stability Analyses	5-6
5.6	Results	5-6
5.7	Remedial Solution	5-12
5.8	Summary and Conclusions	5-12
6.0	Liquefaction Potential Analysis	
6.1	Introduction	6-1
6.1.1	Description of the Project	6-1
6.1.2	Source Materials Required	6-1
6.2	Geological Setting	6-1
6.2.1	Regional Setting	6-1
6.2.2	Local Geology	6-1
6.3	Seismic Design Criteria	6-3
6.4	Probabilistic Seismic Hazard Analysis	6-3
6.5	Geotechnical Information	6-6
6.6	Design of the Embankment	6-6
6.6.1	Design Considerations	6-6
6.6.2	Seismic Slope Stability	6-12
6.6.3	Liquefaction Potential	6-12
6.6.4	Evaluation of the Consequences of Liquefaction	6-15
6.7	Site Response Analyses	6-18
6.8	Detailed Calculations - Example 5 - Liquefaction Potential Analysis	6-18
6.9	Summary and Conclusions	6-42
7.0	References	7-1

CHAPTER 4.0 GROUND MOTION CHARACTERIZATION

4.1 BASIC GROUND MOTION CHARACTERISTICS

Results of the seismic hazard analysis will establish the peak horizontal ground acceleration (PHGA) for use in design analysis. However, PHGA is only one of the characteristics of the earthquake ground motion at a site that influence the potential for damage. The damage potential of seismically-induced ground motions may also depend upon the duration of strong shaking, the frequency content of the motion, the energy content of the motion, peak vertical ground acceleration (PVGA), peak ground velocity and displacement, and the intensity of the motion at times other than when the peak acceleration occurs, as elaborated below.

The acceleration response spectrum is one commonly used index of the character of earthquake ground motions. An acceleration response spectrum provides quantitative information on both the intensity and frequency content of the acceleration time history. However, while widely used in structural engineering, response spectra are of limited use in geotechnical analysis. The primary application of response spectra to geotechnical practice is as an aid in selection of time histories for input to site response and deformation analyses, for comparison of accelerograms, and for illustration and evaluation of the influence of local soil conditions on ground motions.

Other parameters used less frequently than PHGA and the acceleration response spectrum to describe the character of earthquake ground motions include various measures of the duration and energy content of the acceleration time history. Duration is sometimes expressed directly as the length of time from the initiation of strong shaking to its cessation. Alternatively, indirect measures of duration, including the number of equivalent cycles and the number of positive zero crossings of the acceleration time history, are sometimes employed in earthquake engineering practice.

The energy content of the strong ground motion may be expressed in terms of the *root-mean-square* (RMS) and duration of the acceleration time history or in terms of the Arias intensity. The RMS, discussed in detail in Section 4.4, represents an “average” or representative value for the acceleration over the defined duration of the strong ground motion. The Arias intensity is the square of the acceleration integrated over the duration of the motion. The time history of the normalized Arias intensity, referred to as a Husid plot, is sometimes used to define the duration of strong shaking.

These various indices of the character of strong ground motions (*ground motion parameters*) commonly used in engineering practice are defined and described in this chapter. Following their definition and description, procedures for using these indices for selection of representative time histories to characterize earthquake ground motions at a site are presented.

4.2 PEAK VALUES

4.2.1 Evaluation of Peak Parameters

Peak horizontal ground acceleration (PHGA) is the most common index of the intensity of strong ground motion at a site. The PHGA is directly related to the peak inertial force imparted by strong shaking to a structure founded on the ground surface and to the peak shear stress induced within the ground itself. Peak vertical ground acceleration (PVGA), peak horizontal ground velocity (PHGV), and peak horizontal

ground displacement (PHGD) are also used in some engineering analyses to characterize the damage potential of ground motions. For instance, PHGV is a common index of structural damage and PHGD may be used in analyses of retaining walls, tunnels, and underground pipelines. PVGA is an important parameter in the design of base-isolated structures.

Peak values for design analyses are evaluated on the basis of the seismic hazard analysis. For major projects, a site or project specific seismic hazard analysis may be performed. Alternatively, results from published regional seismic hazard analyses or from seismic hazard analyses performed for previous projects in the same vicinity may be used. Most published seismic hazard maps tend to be probabilistic in nature. Both deterministic and probabilistic project-specific analyses are used in practice.

4.2.2 Attenuation of Peak Values

A key step in both deterministic and probabilistic seismic hazard analyses is calculation of the ground motion parameter of interest at a given site from an earthquake of a given magnitude and site-to-source distance. These ground motion parameter values are typically evaluated using an *attenuation relationship*, an equation that relates the parameter value to the key variables on which the ground motion parameter depends (e.g., earthquake magnitude, site-to-source distance, style of faulting). Attenuation relationships may be developed either from statistical analyses of values observed in previous earthquakes or from theoretical models of the propagation of strong ground motions. These observations and analyses indicate that the most important factors influencing peak values of earthquake strong ground motions at a site are the magnitude of the earthquake, the distance between the site and the earthquake source, the style of faulting, and local ground conditions (e.g., rock or soil site conditions).

There are many different attenuation relationships that have been proposed. Campbell (1985), Joyner and Boore (1988), and Atkinson and Boore (1990) provide excellent summaries of many of the available attenuation relationships.

A large number of attenuation relationships are available for the western United States. These attenuation relationships are based primarily on statistical analysis of recorded data. For the eastern and central United States, where little to no recorded strong motion data are available for statistical analysis, relatively few attenuation relationships are available. The few attenuation relationships that do exist for the eastern and central United States are based primarily upon theoretical models of ground motion propagation due to the lack of observational data.

Even when restricted to a relatively narrow geographic locale like the northwestern United States, there may still be a need to use different attenuation relationships for different tectonic conditions. For example, Youngs, *et al.* (1988) found differences in attenuation of ground motions between earthquakes occurring along the interface between the subducting Juan de Fuca tectonic plate and the North American plate (interplate events) and earthquakes occurring within the subducting Juan de Fuca plate (intraplate events) in the Pacific northwest (see Figure 2-1).

PHGA attenuation relationships for shallow earthquakes that occur at the interface between the Pacific and American tectonic plates in the western United States have been developed by many investigators, including Campbell and Duke (1974), Campbell (1993), Campbell and Bozorgnia (1994), Boore, *et al.*, (1993), Boore and Joyner (1994), Sadigh, *et al.*, (1993), Geomatrix (1995), Silva and Abrahamson (1993), Abrahamson and Silva (1996), and Idriss (1995). Table 4-1 presents a summary of commonly used PHGA attenuation relationships in the western United States. These relationships consider earthquake magnitude, site-to-source distance, and local ground conditions (soil or rock). These relationships may also

TABLE 4-1
ATTENUATION RELATIONSHIPS FOR THE WESTERN UNITED STATES
(For Shallow Crustal Earthquakes)

Reference ⁽¹⁾	Magnitude Measure ⁽²⁾	Distance Measure ⁽³⁾	Limitation ⁽⁴⁾
Schnabel and Seed (1973)	M ⁽⁵⁾	Closest Horizontal Distance to the Zone of Energy Release, R_E	Available only in the form of charts. $3 \leq R_E \leq 1,000$ km
Campbell and Duke (1974)	M_S	Hypocentral Distance, R_H	Attenuation of I_A only. $15 \leq R_H \leq 110$ km
Kavazanjian, <i>et al.</i> (1985a)	M_w	Closest Distance to the Rupture Zone, R_R	Attenuation of RMSA only. $0 < R_R < 100$ km
Idriss (1993; 1995)	M_L if $M < 6$ M_S if $M > 6$	Closest Distance to the Rupture Zone, R_R	$1 \leq R_R \leq 60$ km
Joyner and Boore (1988); Boore, <i>et al.</i> (1993)	M_w	Closest <i>Horizontal</i> Distance to the Vertical Projection of the Rupture Zone, R_{JB}	$0 < R_{JB} \leq 80$ km
Geomatrix (1991, 1995); Sadigh, <i>et al.</i> (1993); Silva and Abrahamson (1993); Abrahamson and Silva (1996)	M_w	Closest Distance to the Rupture Zone, R_R	$0 < R_R \leq 100$ km
Campbell (1990; 1993); Campbell and Bozorgnia (1994)	M_L if $M < 6$ M_S if $M > 6$	Seismogenic Distance, R_S	$0 < R_S \leq 60$ km

- Notes: (1) Table lists main references and their latest updates. The following references also include coefficients for spectral values: Joyner and Boore (1988); Geomatrix (1991, 1995); Campbell (1990, 1993); and Idriss (1993). Relationship by Schnabel and Seed (1973) is shown by dashed lines in Figure 4-2. Relationship by Kavazanjian, *et al.* (1985) is shown in Figure 4-7. See Equation 4-4 for Campbell and Duke (1974) relationship.
- (2) M_w = Moment Magnitude, M_L = Local (Richter) Magnitude, M_S = Surface Wave Magnitude. Note that for $M < 6$, $M_L \approx M_w$ and for $M > 6$, $M_S \approx M_w$.
- (3) Refer to the original references for detailed definition of distance measures. Note that for design, it is commonly assumed that the rupture zone equals to the area of the fault plane.
- (4) I_A = Arias Intensity, as defined in Chapter 4.5; RMSA = Root Mean Square Acceleration as defined in Chapter 4.4.
- (5) Magnitude measure was not specified by Schnabel and Seed (1973).

discriminate on the basis of style of faulting, as statistical analysis shows that reverse (thrust) fault events generate peak ground accelerations approximately 20 to 30 percent greater than strike-slip events of the same magnitude at the same distance. Figure 4-1 compares mean value PHGA attenuation curves for magnitude 6.5 and 8.0 events on a strike-slip fault calculated by three commonly used attenuation relationships for western United States earthquakes.

Different attenuation relationships than those used for shallow crustal earthquakes are used for the subduction zone earthquakes that occur along the Pacific Coast in Alaska, Washington, Oregon, and the northwest corner of California. For subduction zone earthquakes, PHGA attenuation relationships by Cohee, *et al.*, (1991) and Youngs, *et al.*, (1988) are often used in earthquake engineering practice. Table 4-2 presents the relationships for attenuation of PHGA in subduction zone earthquakes developed by Cohee, *et al.* (1991) and Youngs, *et al.* (1988).

With respect to differences in ground motion attenuation between the western United States and the eastern and central United States, it is generally agreed that ground motions east of the Rocky Mountains attenuate more slowly than ground motions in the west. However, due to the much lower rates of seismicity and the absence of large magnitude earthquakes since the deployment of strong motion accelerographs in the eastern and central United States, there is insufficient data to characterize the attenuation of strong ground motions east of the Rocky Mountains using statistical methods. Therefore, attenuation relationships used for earthquakes occurring in eastern and central United States are based upon theoretical modeling of ground motion attenuation. Attenuation relationships for the eastern and central United States commonly used in engineering practice include relationships developed by Nuttli and Herrmann (1984), Boore and Atkinson (1987), McGuire, *et al.* (1988), Boore and Joyner (1991), and Atkinson and Boore (1995).

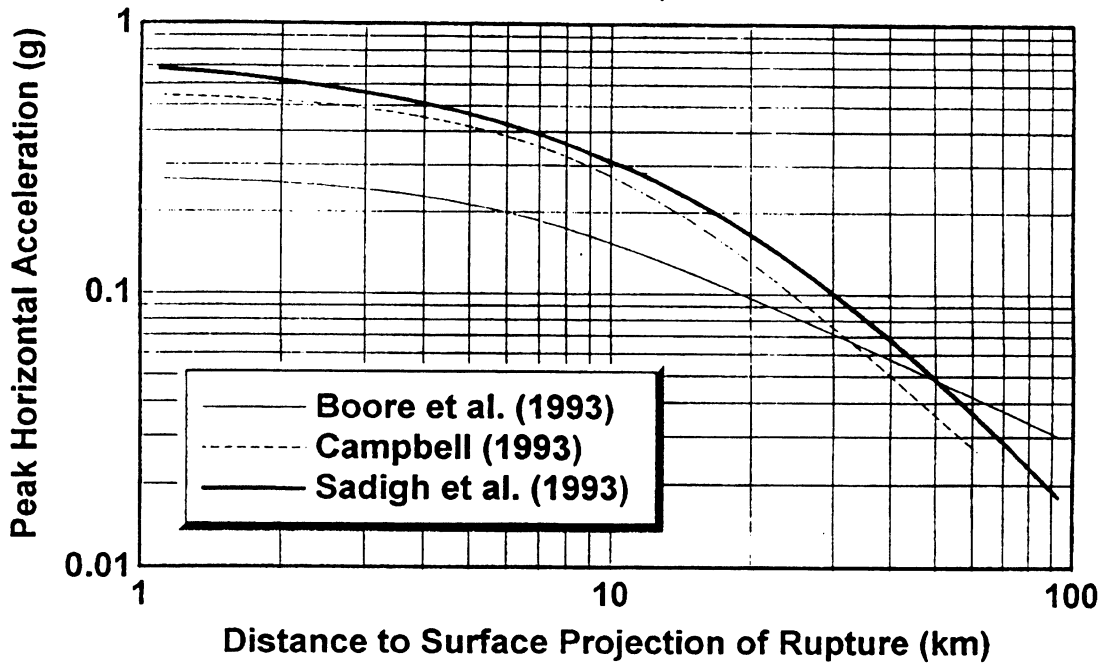
Table 4-2 includes the PHGA attenuation relationships developed by Toro, *et al.* (1997) for the Mid-Continent and Gulf Coast regions that were used in developing the 1996 USGS seismic hazard maps. Figure 4-2 compares typical PHGA attenuation relationship for the eastern and central United States to that used in the western United States (dashed lines).

Factors other than distance, magnitude, and style of faulting may influence the attenuation of strong ground motions. These factors include depth of earthquake hypocenter, the strike and dip of the fault plane (see Figure 2-6), location of the site relative to the hanging and foot walls of a thrust fault (see Figure 2-7), rupture directivity effects, topographic effects, depth to crystalline bedrock, velocity contrasts, asperities on the rupture surface, wave reflection, wave refraction, and wave scattering. Figure 4-3 presents a recent attenuation relationship developed by Abrahamson and Silva (1996) for reverse (thrust) faults showing the influence of the location of the site with respect to the hanging wall and the foot wall of the fault. Most other factors (e.g., directivity, rupture effects) are not explicitly considered in attenuation relationships and can only be accounted for by detailed seismologic modeling.

4.2.3 Selection of Attenuation Relationships

The engineer choosing an attenuation relationship for use in practice should keep in mind that new attenuation relationships are regularly being developed. Many of the investigators who have developed attenuation relationships for the western United States revise their relationships after almost ever major earthquake to include newly recorded motions. Therefore, when selecting an attenuation relationship, it is prudent to review the current literature and select the most appropriate relationship or relationships for the project site. When evaluating whether or not a certain attenuation relationship is appropriate, the engineer should thoroughly review the published information regarding its development, especially the tectonic regime for which it was developed, the ranges of magnitude and distance to which it is restricted,

ROCK SITE; $M_w = 6.5$



ROCK SITE; $M_w = 8.0$

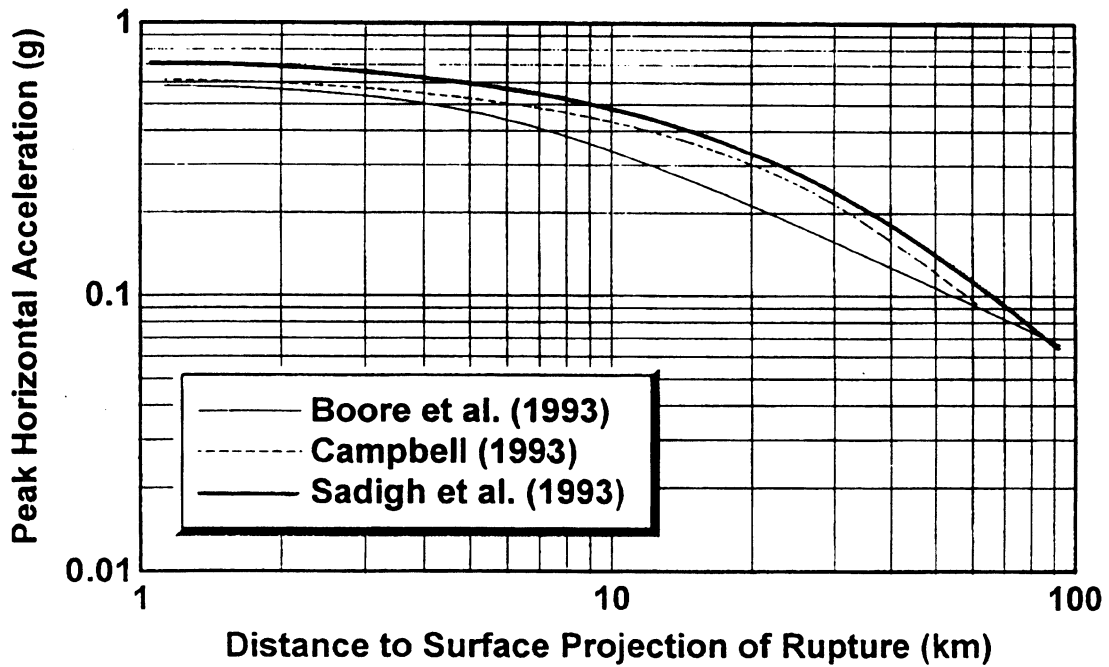


Figure 4-1: Comparison of Attenuation Relationships by Various Investigators. (For Strike-Slip Faults)

TABLE 4-2
ATTENUATION RELATIONSHIP FOR SUBDUCTION ZONE AND CENTRAL
AND EASTERN UNITED STATES EARTHQUAKES

Reference	Attenuation Relationship	Limitation ⁽¹⁾
Subduction Zone Youngs, <i>et al.</i> (1988)	$\ln(\text{PGA}) = 19.16 + 1.045M_w - 4.738 \ln[R_H + 205.5 \exp(0.0968M_w)] + 0.54Z_t$	$20 < R_H \leq 40 \text{ km}$ $M_w \leq 8$
Subduction Zone Youngs, <i>et al.</i> (1988)	$\ln(\text{PGA}) = 19.16 + 1.045M_w - 4.738 \ln[R_H + 154.7 \exp(0.1323M_w)]$	$20 < R_H \leq 40 \text{ km}$ $M_w > 8$
Subduction Zone Cohee, <i>et al.</i> (1991)	$\ln(\text{PGA}) = 1.5 - 3.33 \ln(R_S + 128) + 0.79s$	$25 < R_S < 175 \text{ km}$ $M_w \leq 8$
Subduction Zone Cohee, <i>et al.</i> (1991)	$\ln(\text{PGA}) = 2.8 - 1.26 \ln(R_R) + 0.79s$	$30 < R_R < 100 \text{ km}$ $M_w > 8$
Mid-Continent Toro, <i>et al.</i> (1997)	$\ln(\text{PGA}) = 2.20 + 0.81 (M_w - 6) - 1.27 \ln(R_m) - 0.11 \text{ Max}[\ln (R_m/100), 0] - 0.0021 R_m$	
Gulf Coast Toro, <i>et al.</i> (1997)	$\ln(\text{PGA}) = 2.80 + 1.31 (M_w - 6) - 1.49 \ln(R_m) - 0.09 \text{ Max}[\ln (R_m/100), 0] - 0.0017 R_m$	

Notes: M_w = Moment magnitude.
 R_H = Hypocentral distance.
 R_R = Closest distance to the rupture zone (fault plane).
 R_S = Seismogenic distance (closest distance from the fault asperity).
 R_m = $\sqrt{R_{JB}^2 + C_J^2}$
 C_J = 9.3 for Mid-Continent, 10.9 for Gulf Coast
 R_{JB} = Closest Horizontal Distance to Vertical Projection of Fault Plane (see Figure 2-7)
 Z_t = The tectonics term in Youngs, *et al.* (1988). Equal to 0 for interplate events, and 1 for intraplate events.
 s = The site term in Cohee, *et al.* (1991) relationship. Equal to 0 for rock sites and 1 for soil sites.
⁽¹⁾ = Refer to the original references for detailed description of distance measures and limitations.

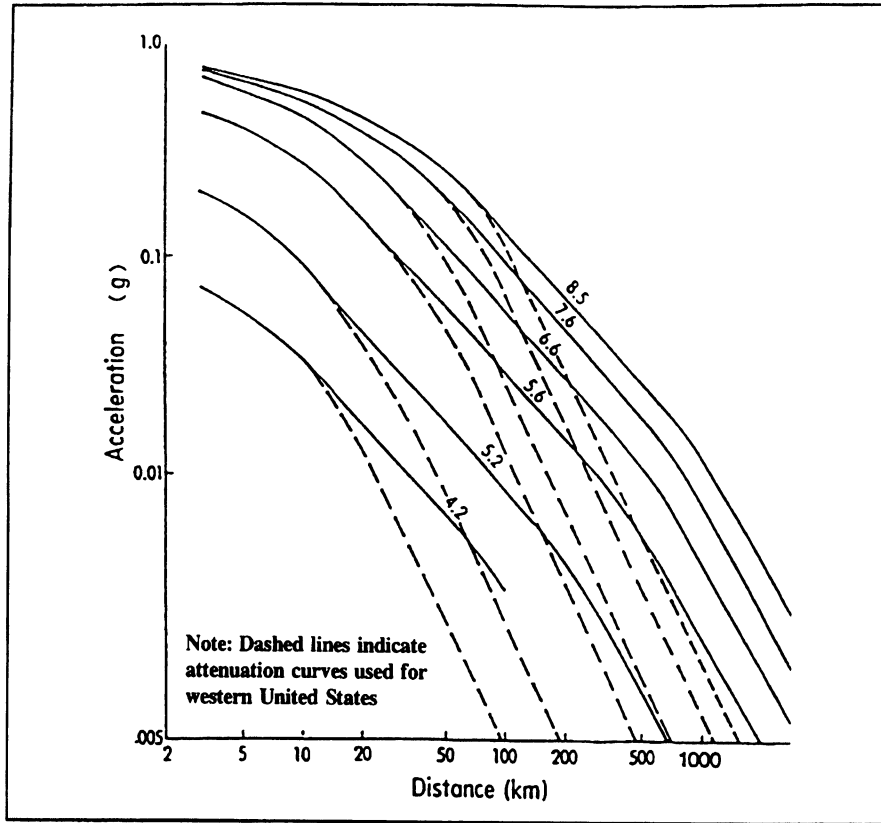


Figure 4-2: Comparison of Attenuation Relationship for Eastern and Central United States to Attenuation Relationship for Western United States.

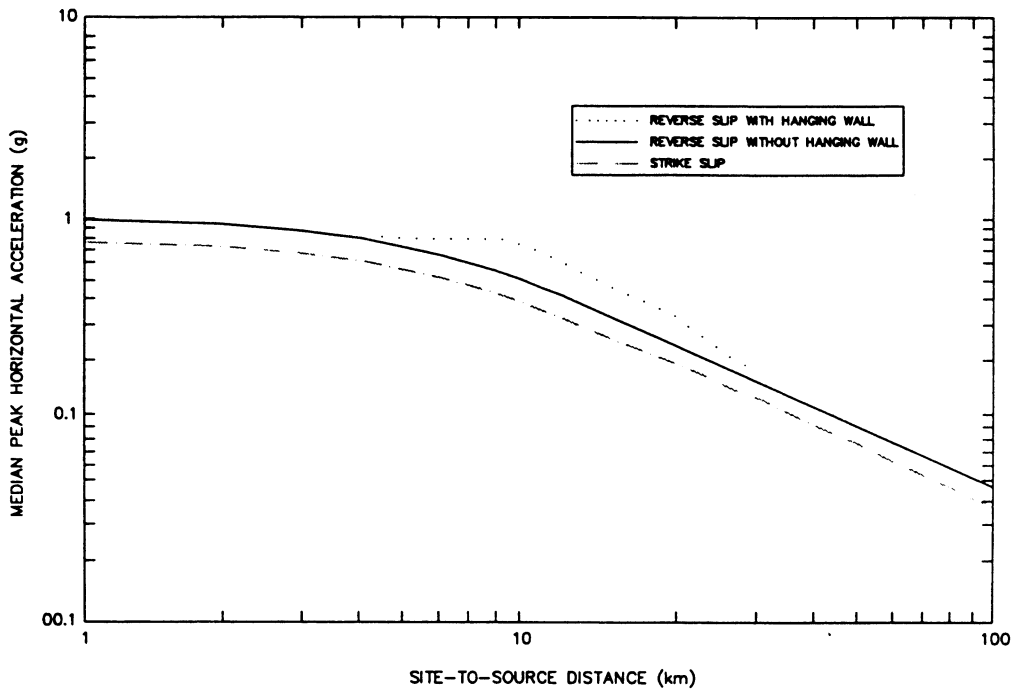


Figure 4-3: Abrahamson and Silva (1997) Attenuation Relationship

and the local ground conditions to which it applies. Frequently, several different attenuation relationships may be found to be equally appropriate. In such a case, the geometric mean (i.e., $\ln X_{\text{mean}} = (\sum \ln X_i)/n$) of the values calculated using all of the appropriate attenuation relationships is commonly employed in practice. By using the geometric mean of the values calculated by multiple relationships, bias inherent to individual relationships is minimized. However, when this approach is used, the multiple attenuation relationships *should not* include two generations of an attenuation relationship from the same investigator (e.g., Campbell, 1989 and Campbell and Bozorgnia, 1994).

Usually, attenuation relationships for both rock and soil sites will be available for use. Except for soil sites with less than 10 m of soil overlying bedrock and for soft soil sites where the average shear wave velocity over the top 30 m is less than 120 m/s, soil-site attenuation relationships may be used directly to characterize ground motions at a soil site. However, due to the variability in conditions at soil sites and the resulting uncertainty in soil site response, engineers often prefer to use a rock site attenuation relationship to characterize the design earthquake motions at a *hypothetical bedrock outcrop* at the geometric center of the project site and then conduct a site response analysis to evaluate the influence of local soil conditions on the earthquake motions at the site. The hypothetical bedrock outcrop concept is congruent with both the *free-field* (i.e., not affected by structure and/or topography) criterion used to develop the attenuation relationships and with the concepts used to specify motions for input to computer programs for seismic site response analyses (rock outcrop and transmitting boundary models, see Sections 6.4 and 6.5).

4.2.4 Selection of Attenuation Relationship Input Parameters

When using an attenuation relationship, it is important to use the magnitude scale consistent with the scale used to develop the attenuation relationship. In the eastern and central United States, the magnitude measure generally used in practice is body wave magnitude, m_b . In California, moment magnitude, M_w , local (Richter) magnitude, M_L , or surface wave magnitude, M_s , are used. The differences in these scales are due to the type of earthquake waves being measured, the type of instrument used to measure them, and local scaling factors. The relationship between these magnitude scales is shown on Figure 2-5.

Consistency with the site-to-source distance measure used in developing the attenuation relationship is also important, especially for near-field earthquakes. In the early days of development of attenuation relationships, the epicentral distance was often used because it was generally the most reliable distance measure (seismographs were too sparsely located to adequately constrain the focal depth). As seismographs became more numerous and portable arrays were deployed to measure aftershock patterns that roughly delineate the rupture zone, the focal depth and extent of the rupture surface were able to be better located. Statistical analyses indicate that measures of distance from the recording site to the rupture surface provide a more robust measure of seismic wave attenuation than epicentral distance. Therefore, most current attenuation relationships for the western United States use some measure of the distance to the rupture zone. In the eastern and central United States, hypocentral and epicentral distance measures are still commonly used due to the sparsity of strong-motion recordings from significant earthquakes.

4.2.5 Distribution of Output Ground Motion Parameter Values

All of the attenuation relationships commonly used in practice assume that the output ground motion parameter values are log-normally distributed (i.e., the logarithm of the parameter value is normally distributed). Most of the traditional attenuation relationships used in practice characterize the distribution of the output parameter values with a single, constant value for the log normal standard deviation, independent of earthquake magnitude. In these traditional relationships, the mean plus one standard

deviation peak acceleration values are typically about 1.5 times the corresponding mean values. Recently, Sadigh, *et al.* (1993), Idriss (1993), and Campbell and Bozorgnia (1994) have developed magnitude dependent values for the standard deviation, with smaller standard deviations for larger magnitudes.

4.3 FREQUENCY CONTENT

The importance of the frequency content of the earthquake ground motions with respect to the damage potential of the motions has been demonstrated repeatedly by damage surveys following earthquakes. Such damage surveys show strong correlations between damage to engineered structures, the natural period of the damaged structure, and the predominant frequency of the ground motion to which the structure was subjected. The frequency content of earthquake ground motions is generally characterized by the shape of the acceleration response spectrum. Velocity and displacement response spectra are also used in practice to characterize the frequency content of ground motions.

The same statistical analyses used to develop peak ground motion attenuation equations for the western United States have been used to develop attenuation relationships for spectral values. Joyner and Boore (1988), Geomatrix (1991), Campbell (1993), and Idriss (1993) present the coefficients for spectral acceleration attenuation for spectral periods of up to 7.5 seconds. These coefficients can be used to generate smoothed response spectra that illustrate the influence of magnitude and distance on the frequency content of strong ground motions.

Figure 4-4 compares smoothed acceleration response spectra for a rock site from Campbell (1993) for magnitude 5.5, 6.5, and 7.5 events at a distance of 15 km. For comparison purposes, these spectra are all normalized to a zero period (peak ground) acceleration value of 1.0. This figure clearly illustrates the increased damage potential of larger magnitude earthquakes. The larger magnitude events have larger peak spectral accelerations and larger spectral accelerations in the long period range where ground motions are often most damaging, even though all three spectra are scaled to the same peak acceleration value.

Figure 4-5 compares smoothed acceleration response spectra from three different investigators (Campbell, 1993; Sadigh, *et al.*, 1993; and Boore, *et al.*, 1993) for a rock site for a magnitude 6.5 event at a distance of 15 km. This figure illustrates the differences among attenuation relationships developed by different investigators using essentially the same data base. These differences are primarily due to the weighting scheme used in statistical analysis and the screening criteria used by each investigator in culling records from the common data base of world-wide strong motion records available for the analysis and theoretical assumptions on the shape of the attenuation relationship in the near field (whether or not it "saturates" (plateaus) at low distances) and the rate of decay of ground motion in the far field. The decision on which attenuation to use is a subjective one that is generally based on a comparison between the data base and assumptions used to develop the attenuation relationship and the problem at hand. Alternatively, the arithmetic average or geometric mean of multiple attenuation relationships may be used.

The smoothed acceleration response spectra illustrated in Figures 4-4 and 4-5 are important tools for selection of appropriate time histories for geotechnical analysis. When selecting or synthesizing ground motion time histories for use in engineering analysis, the smoothed spectra are used as a guide to the appropriateness of the time history frequency content. As illustrated in Figure 4-6, a suite of time histories for use in engineering analysis is selected such that the suite as a group conforms to the smoothed spectra, though no single time history is expected to conform to the spectra.

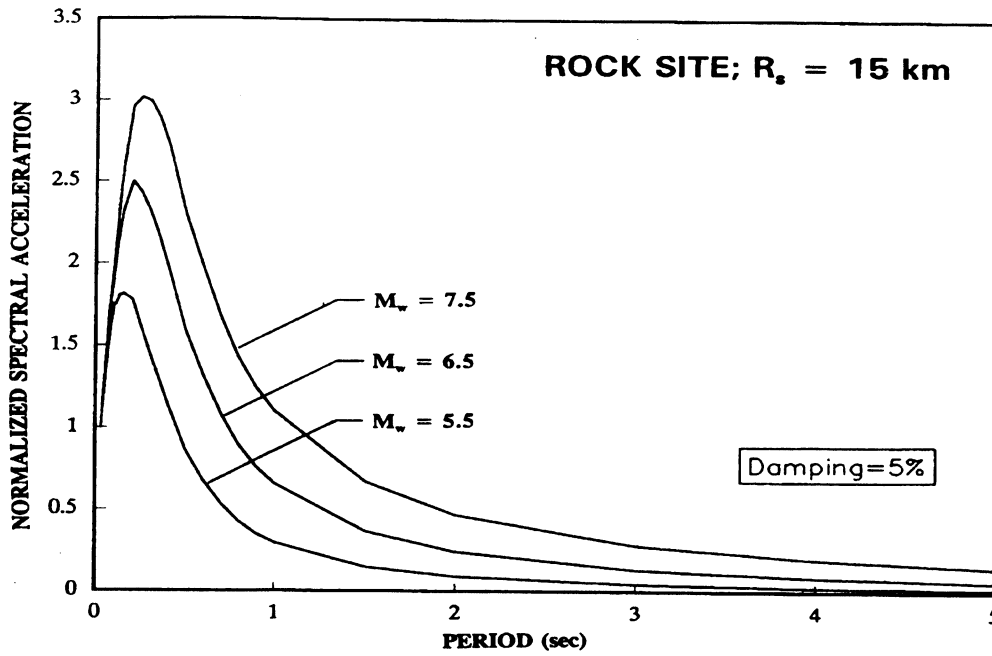


Figure 4-4: Comparison of Smoothed Acceleration Response Spectra for Various Earthquake Magnitudes. (Campbell, 1993 Attenuation Relationship)

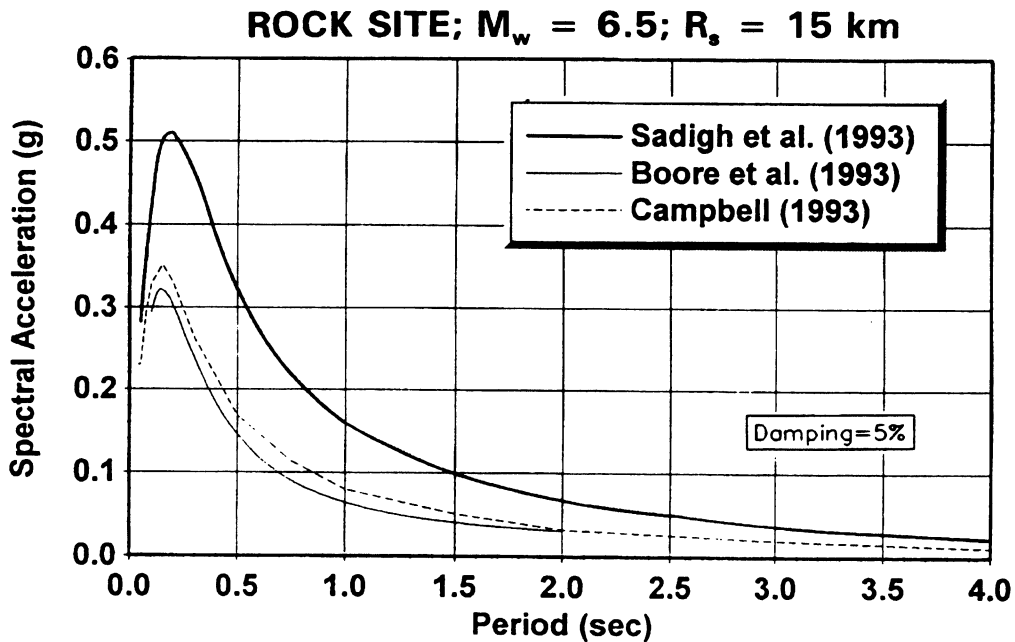


Figure 4-5: Comparison of Smoothed Acceleration Response Spectra by Various Investigators.

**OII LANDFILL
MONTEREY PARK, CALIFORNIA**

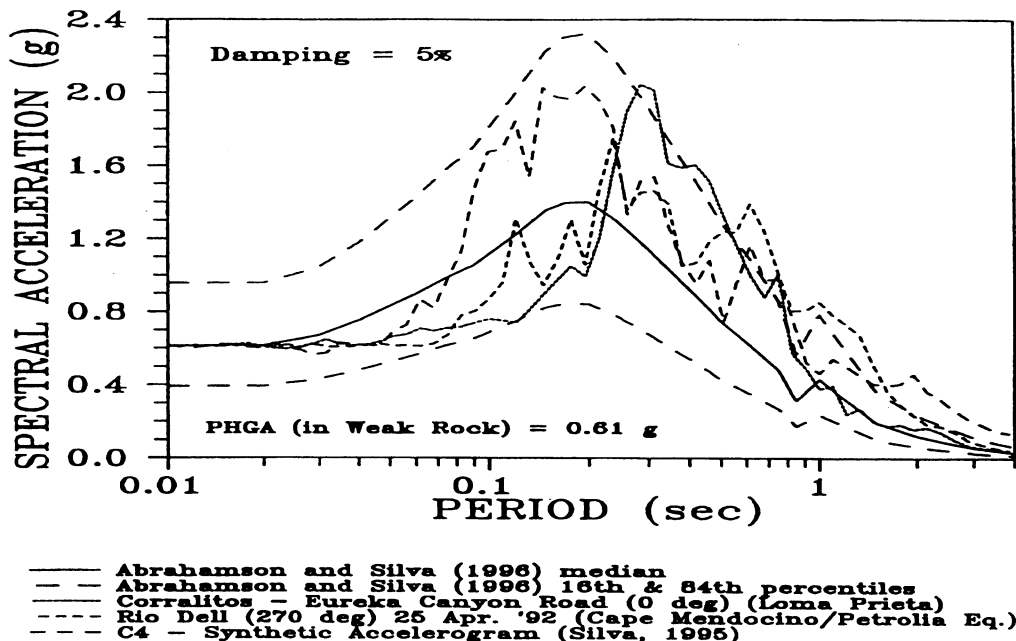


Figure 4-6: Real Spectra vs. Smoothed Spectra

4.4 ENERGY CONTENT

The *energy content* of the acceleration time history provides another means of characterizing strong ground motions. The energy content of the motion is proportional to the square of the acceleration. In engineering practice, the energy content of the motion is typically expressed in terms of either the *root-mean-square* (RMS) and duration of the acceleration time history or the *Arias intensity*, I_A . The RMS of the acceleration time history is the square root of the square of the acceleration integrated over the duration of the motion and divided by the duration:

$$RMSA = \sqrt{\frac{1}{t_r} \int_{t_{r0}}^{t_r} [a(t)]^2 dt} \quad (4-1)$$

where RMSA is the RMS of the acceleration time history, $a(t)$ is the acceleration time history, and t_r is the duration of strong ground shaking. The RMSA represents an average acceleration for the time history over the duration of strong shaking. The square of the RMSA multiplied by the duration of the motion is directly proportional to the energy content of the motion.

The value of the RMSA depends upon the definition of the duration of the motion. For instance, if the duration of the motion is defined such that it extends into the quiet period beyond the end of strong shaking, the RMSA value will be "diluted" by the quiet period at the end of the record. However, as the energy content of the motion is unchanged, the product of the RMSA and duration will remain constant. As the RMSA is not used as frequently as peak ground acceleration in engineering practice, RMSA attenuation relationships are not developed or revised as frequently as peak acceleration attenuation relationships. Figure 4-7 presents an attenuation relationship for RMSA at rock sites in the western United States developed by Kavazanjian, *et al.* (1985a) using the significant duration (Trifunac and Brady, 1975) defined in the next Section of this Chapter.

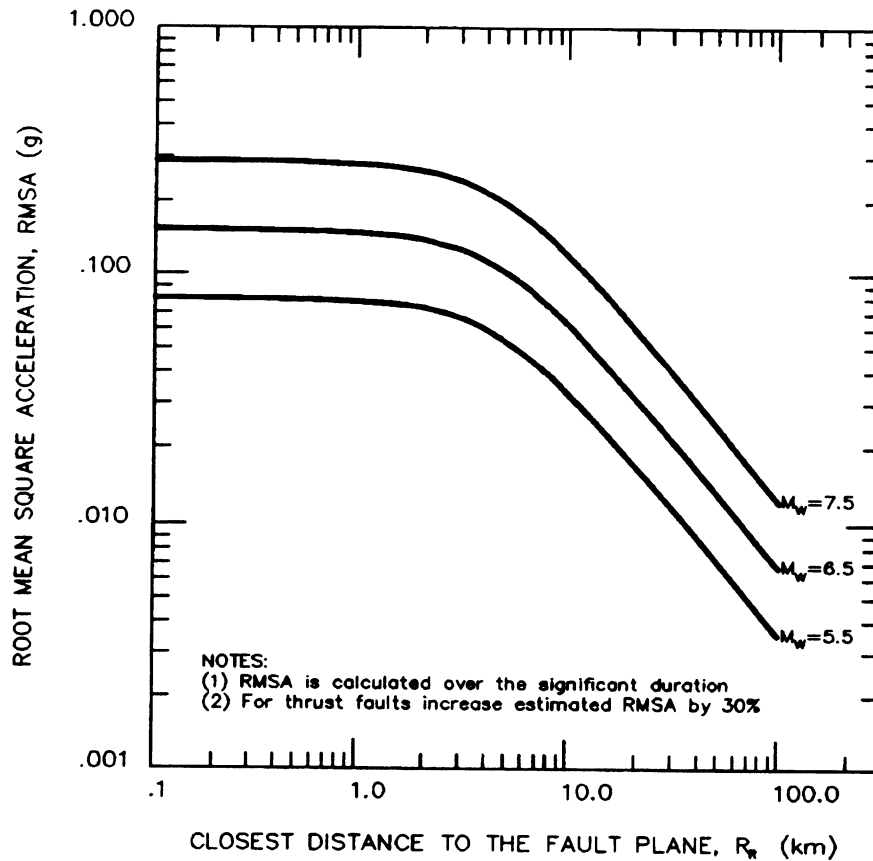


Figure 4-7: Attenuation of the Root Mean Square Acceleration. (Kavazanjian, *et al.*, 1985a, reprinted by permission of ASCE)

The *Arias intensity*, I_A , is proportional to the square of the acceleration integrated over the entire acceleration time history, $a(t)$:

$$I_A = \frac{\pi}{2g} \int_0^{t_f} [a(t)]^2 dt \quad (4-2)$$

where g is the acceleration of gravity and t_f is the duration of strong shaking. Arias (1969) showed that this integral is a measure of the total energy of the accelerogram. Arias intensity may be related to the RMSA as follows:

$$I_A = \frac{\pi}{2g} (\text{RMSA})^2 \cdot t_f \quad (4-3)$$

Figure 4-8 presents the attenuation relationship developed by Kayen and Mitchell (1997) for Arias intensity.

The specification of the duration of strong shaking for an acceleration time history can be somewhat arbitrary, as relatively low intensity motions may persist for a long time towards the end of the record. If the defined duration of strong motion is increased to include such low intensity motions, the Arias

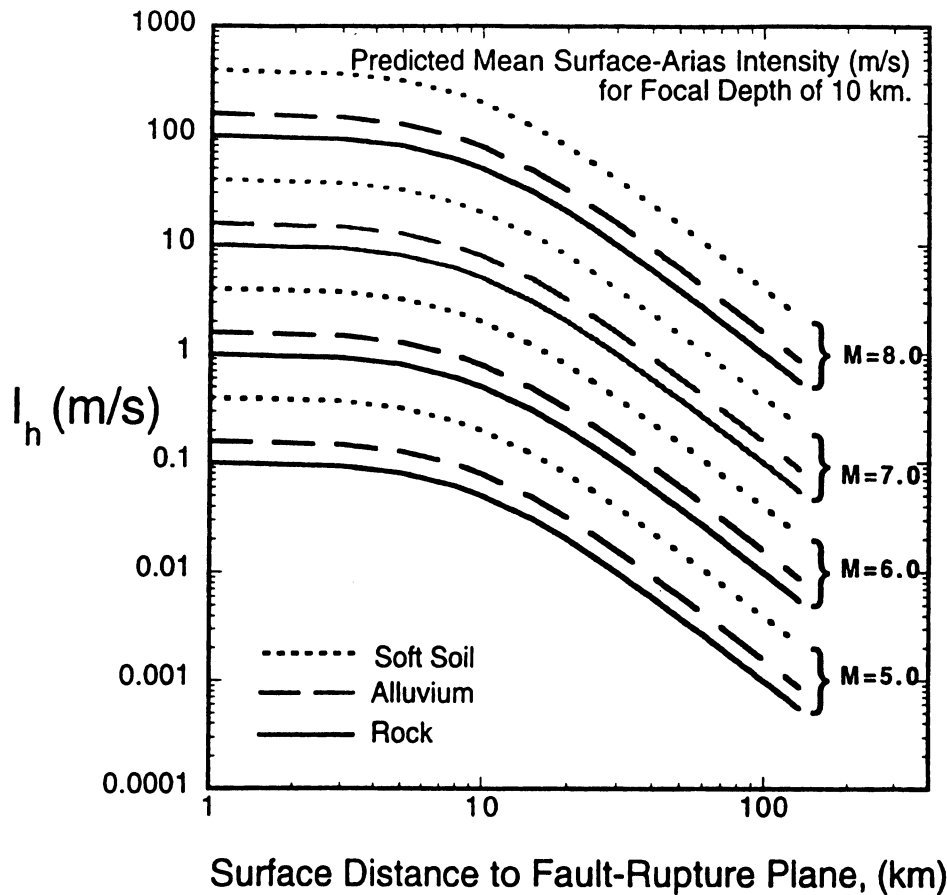


Figure 4-8: Arias Intensity Attenuation Relationship (Kayen and Mitchell, 1997)

intensity will remain essentially constant but the RMSA will decrease (as discussed above). Therefore, some investigators prefer Arias intensity to RMSA as a measure of energy content because the Arias intensity of a strong motion record is a more definite, essentially fixed value while the RMSA depends upon the definition of the duration of strong ground motion. A definition that results in a longer duration will result in a lower RMSA, but I_A will remain essentially unchanged.

Husid (1969) proposed plotting the evolution of the Arias intensity for an accelerogram versus time to study the evolution of energy release for the strong motion record. Figure 4-9 presents the acceleration time history recorded at Aloha Avenue in Saratoga during the 1989 M_w 6.9 Loma Prieta earthquake and the corresponding Husid plot.

Arias intensity and/or RMSA and duration are useful parameters in selecting time histories for geotechnical analysis. This is particularly true if a *seismic deformation analysis* is to be performed, as the deformation potential of a strong motion record is directly proportional to the energy content, which can be expressed as a function of either Arias intensity or the product of the RMSA and duration of the record.

4.5 DURATION

The duration of shaking is important to the response of a soil deposit and/or overlying structures if the materials are susceptible to cyclic pore pressure generation, loss of strength or stiffness during cyclic

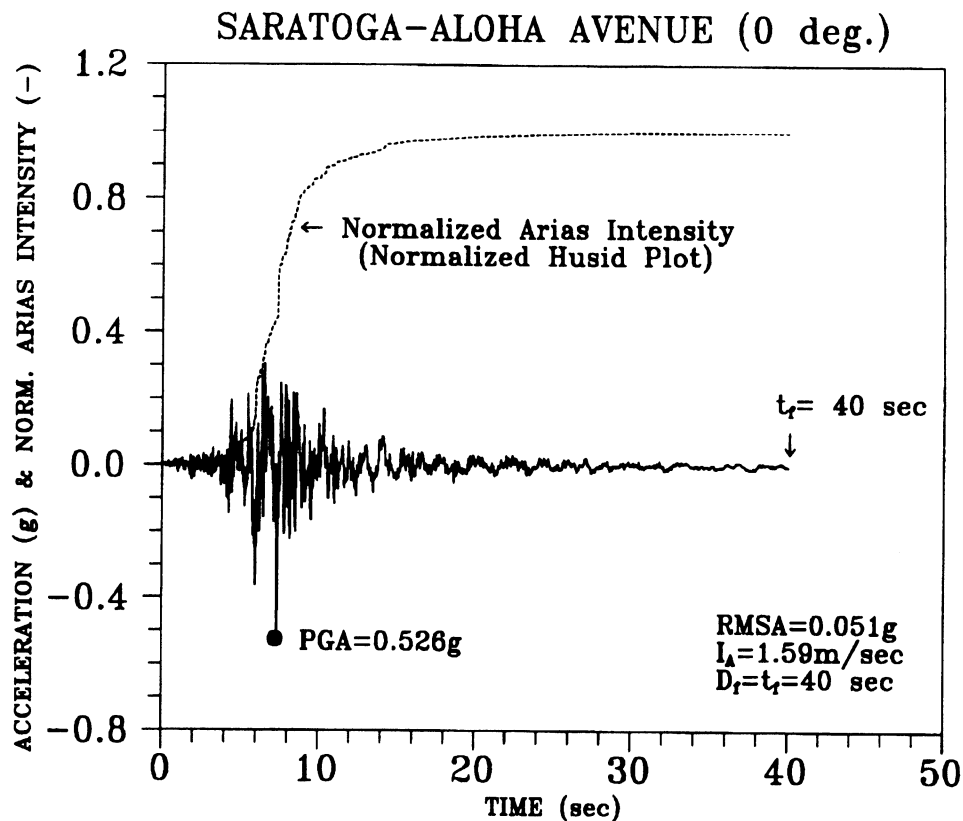


Figure 4-9: Accelerogram Recorded During the 1989 Loma Prieta Earthquake.

loading, or other forms of cumulative damage (e.g., permanent seismic deformation). Duration is often neglected or treated indirectly in evaluating the dynamic response of structures, but is usually implicitly (based upon magnitude) or explicitly accounted for in liquefaction and seismic deformation analyses.

The *bracketed duration of strong motion*, D_b , defined by Bolt (1973) as the elapsed time between the first and last acceleration excursion greater than a specified threshold level, is the definition most often found in strong motion catalogs. Figure 4-10 illustrates calculation of bracketed duration for Saratoga - Aloha Avenue accelerogram and a threshold acceleration of 0.05 g.

For problems dealing with cumulative damage during an earthquake, many engineers find the definition of *significant duration*, D_s , proposed by Trifunac and Brady (1975) to be the most appropriate duration definition. Trifunac and Brady (1975) defined the significant duration as the time interval between 5 and 95 percent of the total Arias intensity on a Husid plot. The Trifunac and Brady definition of duration is illustrated on the Husid plot in Figure 4-11.

The most recent study of significant duration available in the technical literature is by Dobry, *et al.* (1978). These investigators plotted significant duration versus earthquake magnitude for events less than and greater than 25 km from the source. Based upon the summary plot shown on Figure 4-12, these investigators suggested the following design equation for the significant duration at rock sites:

$$D_s = 10^{(0.432M_w - 1.83)} \quad (4-4)$$

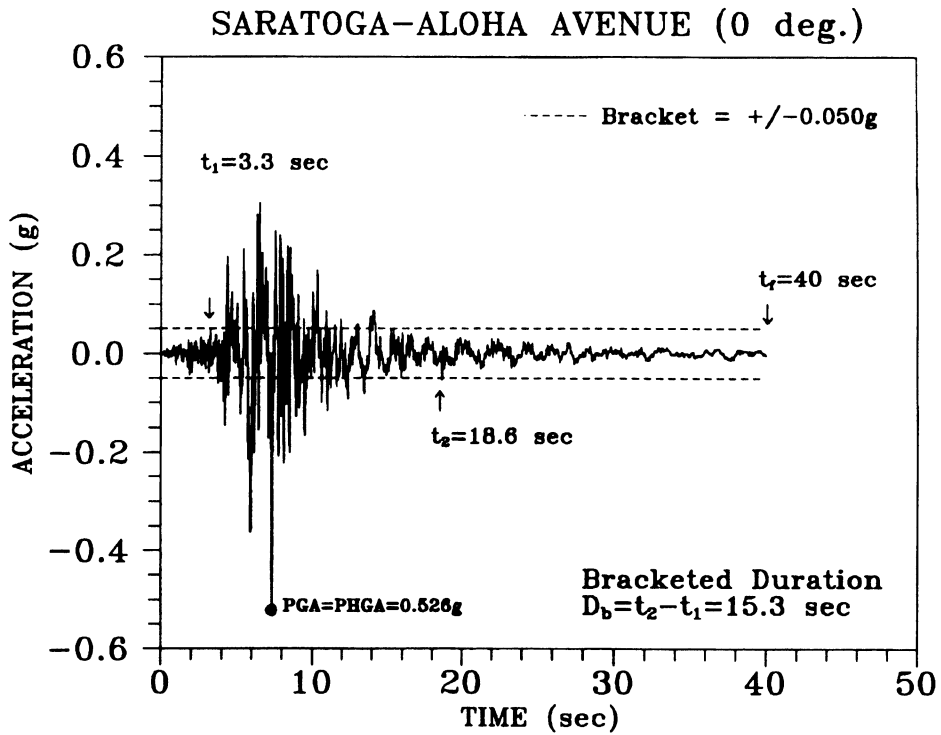


Figure 4-10: Bolt (1973) Duration of Strong Shaking.

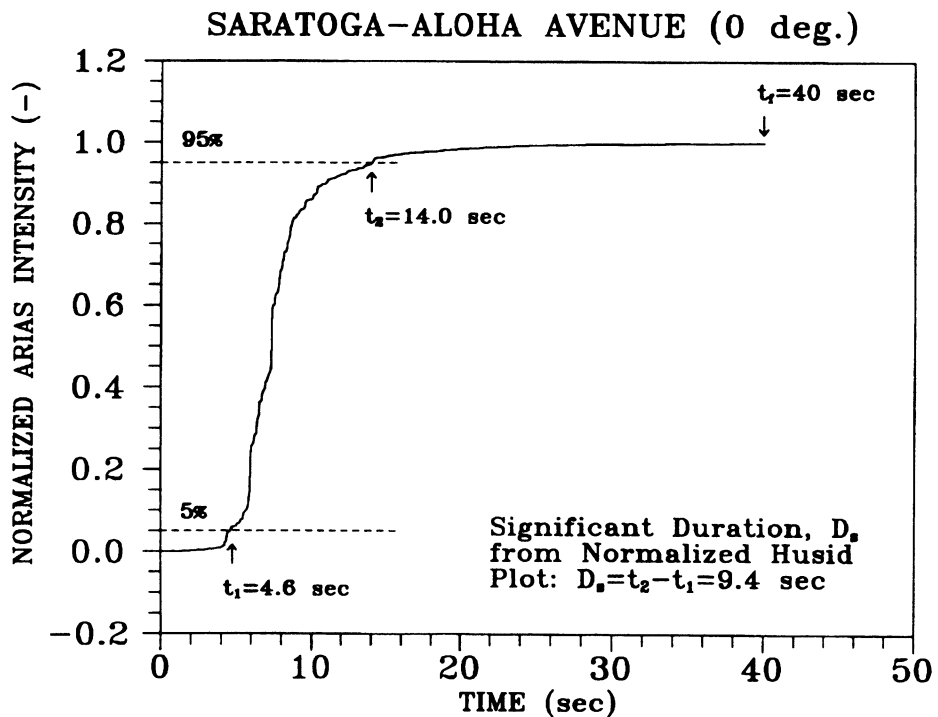


Figure 4-11: Trifunac and Brady (1975) Duration of Strong Shaking.

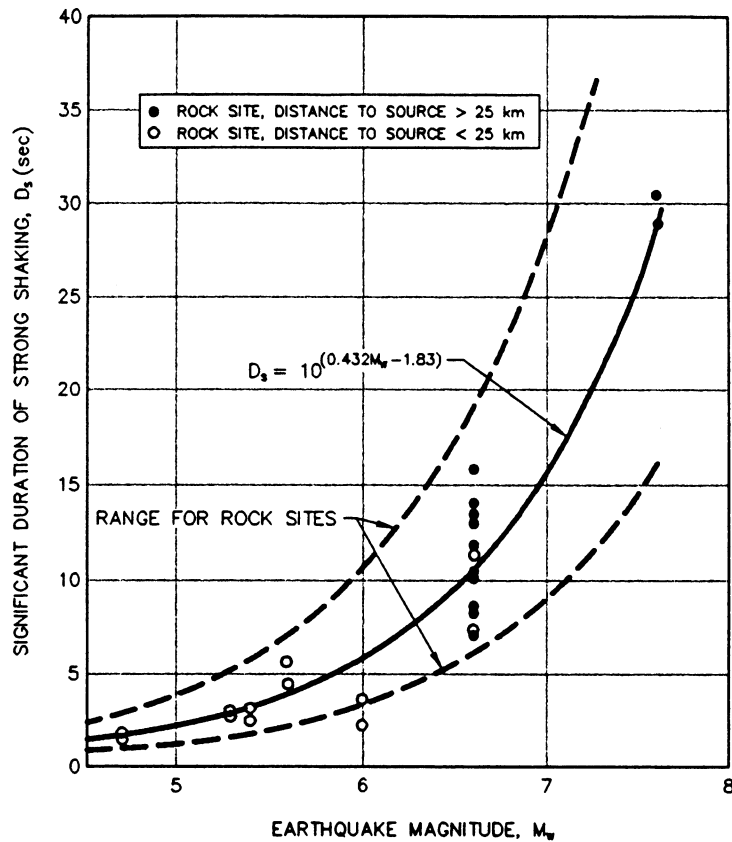


Figure 4-12: Duration Versus Earthquake Magnitude for the Western United States. (Dobry, *et al.*, 1978, reprinted by permission of SSA)

where D_s is the significant duration as defined by Trifunac and Brady (1975) and M_w is the moment magnitude of the design earthquake.

For problems related to soil liquefaction, duration is commonly expressed in terms of the *number of equivalent uniform cycles* (e.g., see Seed, *et al.*, 1975). The number of equivalent uniform cycles is typically expressed as a function of earthquake magnitude to reflect the general increase in duration with increasing magnitude. Recommendations for the number of equivalent uniform cycles as a function of earthquake magnitude for use in liquefaction and seismic settlement analyses are presented in Chapter 8.

4.6 INFLUENCE OF LOCAL SITE CONDITIONS

4.6.1 Local Site Effects

Qualitative reports of the influence of local soil conditions on the intensity of shaking and on the damage induced by earthquake ground motions date back to at least the 1906 San Francisco earthquake (Wood, 1908). Reports of localization of areas of major damage within the same city and of preferential damage to buildings of a certain height within the same local area from the Mexico City earthquake of 1957, the Skopje, Macedonia earthquake of 1963, and the Caracas, Venezuela earthquake of 1967 focused the attention of the engineering community on the influence of local soil conditions on the damage potential of earthquake ground motions.

Back-analysis by Seed (1975) of accelerograms from the moment magnitude M_w 5.3 Daly City (San Francisco) earthquake of 22 March 1957, presented in Figure 4-13, demonstrate the influence of local soil conditions on site response. Figure 4-13 shows peak acceleration, acceleration response spectra, and soil

stratigraphy data at six San Francisco sites approximately the same distance from the source of the 1957 earthquake. The peak acceleration and frequency content of the ground motion recorded at these six sites were dependent on the soil profile beneath each specific site.

At the sites shown in Figure 4-13, the local soil deposits attenuated the peak ground acceleration by a factor of approximately two compared to the bedrock sites. However, the acceleration response spectra for the soil sites clearly show amplification of spectral accelerations at longer periods (periods greater than 0.25 sec) compared to the rock sites. If the bedrock motions had larger spectral accelerations at the longer periods, a characteristic of larger magnitude events and of events from a more distant source, or if the natural period of the local soil deposits more closely matched the predominant period of the bedrock motions, amplification of the peak acceleration could have occurred at the soil sites.

The influence of local ground conditions can also be illustrated using the smoothed acceleration response spectra discussed in Section 4.3. Figure 4-14 presents smoothed acceleration response spectra calculated using the Campbell and Bozorgnia (1994) attenuation relationship for a magnitude 8 event at a distance of 5 km for both soil and rock sites. This figure clearly indicates the tendency for soil site motions to contain a larger proportion of their energy content at longer periods than rock site motions.

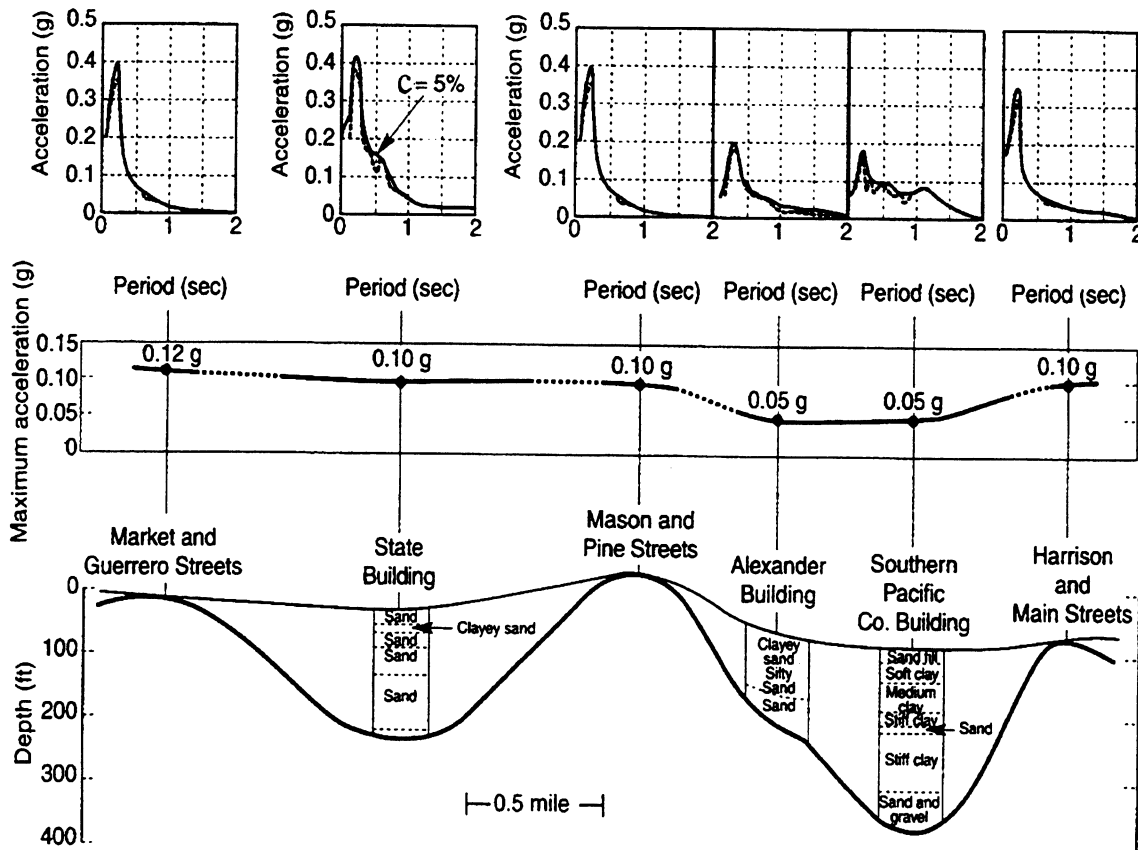


Figure 4-13: Soil Conditions and Characteristics of Recorded Ground Motions, Daly City (San Francisco) M_w 5.3 Earthquake of 1957. (Seed, 1975, reprinted by permission of Chapman and Hall)

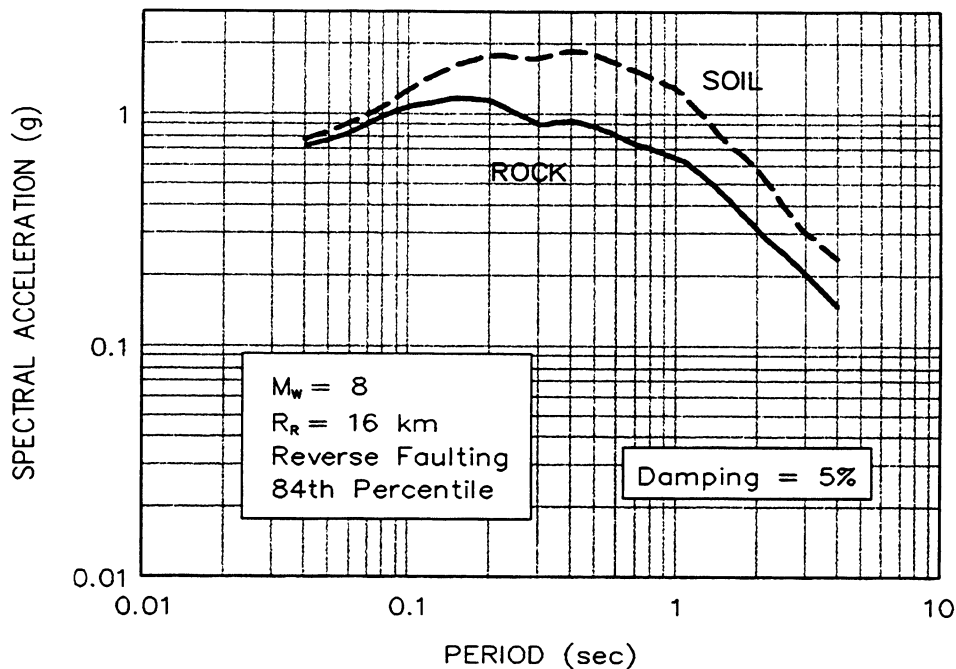


Figure 4-14: Comparison of Soil and Rock Site Acceleration Response Spectra for M_w 8 Event at 5 km. (Campbell and Bozorgnia, 1994, reprinted by permission of EERI)

The Richter Magnitude 8.0 Mexico City earthquake of 1985 provided dramatic evidence of the influence of local soil conditions on earthquake ground motions with respect to both peak ground acceleration and spectral acceleration. Figure 4-15 compares the peak ground acceleration measured at three soft soil sites in Mexico City to the peak acceleration values calculated from a conventional attenuation relationship at the mean plus one standard deviation level. As the figure shows, the peak ground accelerations at the three soft soil sites were significantly greater than the calculated mean plus one standard deviation acceleration values. The peak ground acceleration at one of these sites approached 0.2 g as compared to the mean plus one standard deviation value of 0.08 g for this earthquake, which occurred at a distance of 400 km from Mexico City. Figure 4-16 shows the effect of the local soil conditions at two of these three sites on spectral accelerations. The acceleration response spectra for the two soft clay sites show spectral amplification factors of up to 6 (i.e., a ratio of spectral acceleration to peak ground acceleration of up to 6) at the resonant site period.

4.6.2 Codes and Standards

The influence of local soil conditions on spectral shape may be illustrated using design spectra developed for building codes. For example, the 1994 version of the Uniform Building Code (UBC, 1994), defined three classes of site conditions when defining the shape of the normalized smoothed response spectra for structural design. These three classes of site conditions are rock (Type I), deep, cohesionless or stiff clay soil (Type II), and soft to medium stiff clays and sands (Type III). The smoothed normalized response spectra corresponding to these three site conditions, presented in Figure 4-17, again illustrate the increase in spectral acceleration at long periods for soil site motions compared to rock site motions.

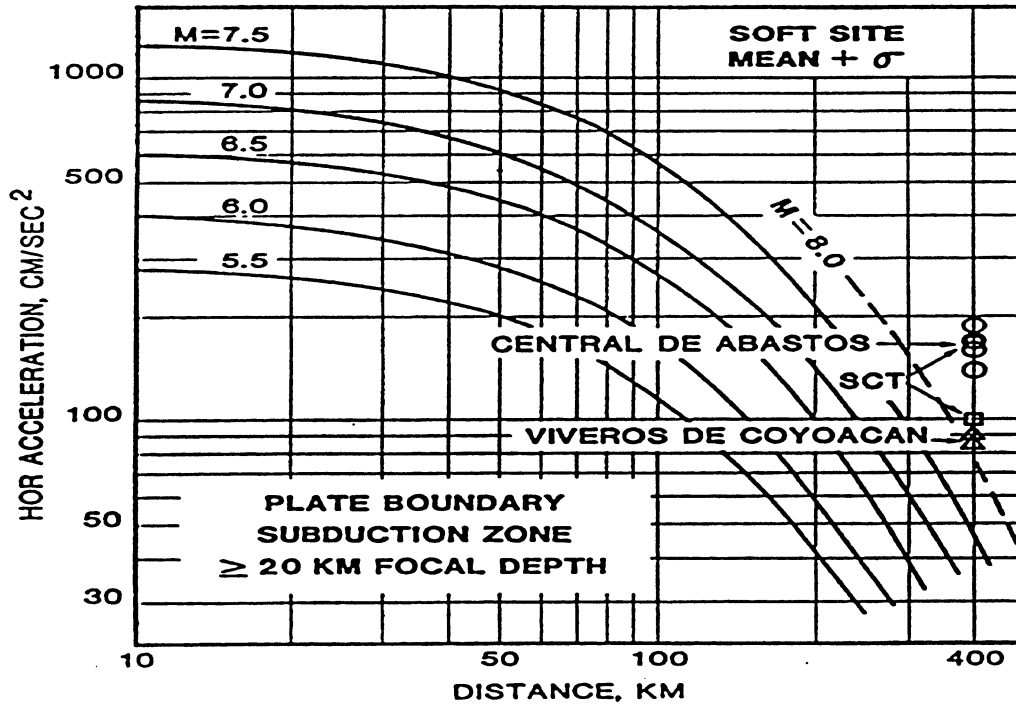


Figure 4-15: PGA Attenuation in 1985 Mexico City Earthquake (Krinitzsky, 1986)

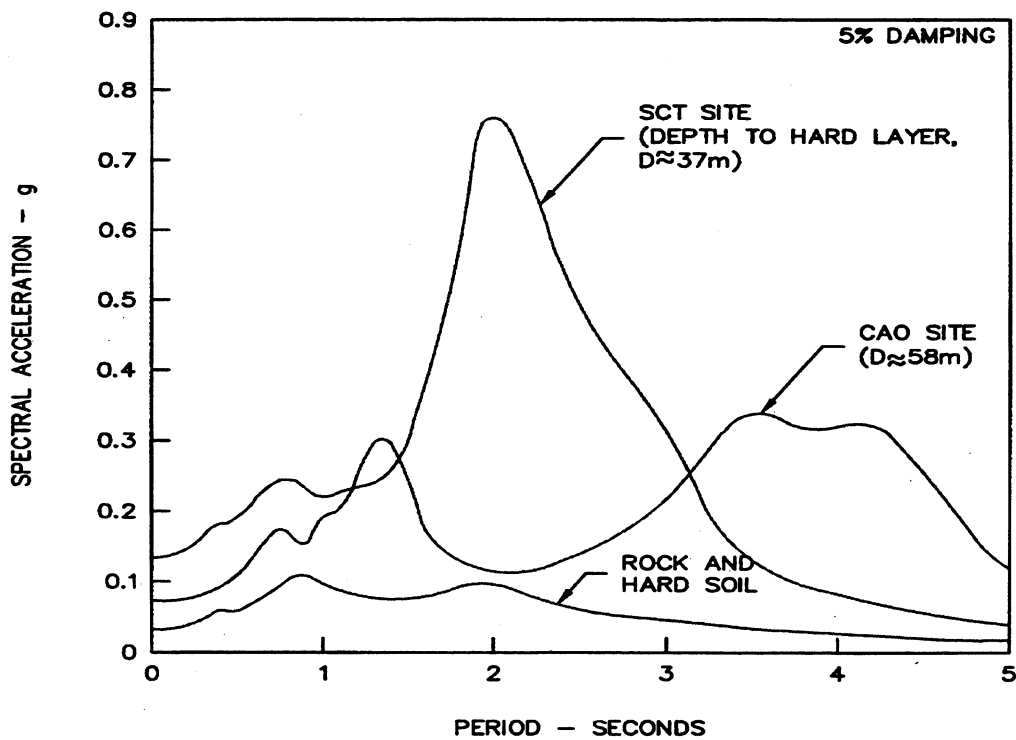


Figure 4-16: Spectral Amplification in 1985 Mexico City Earthquake (Romo and Seed, 1986)

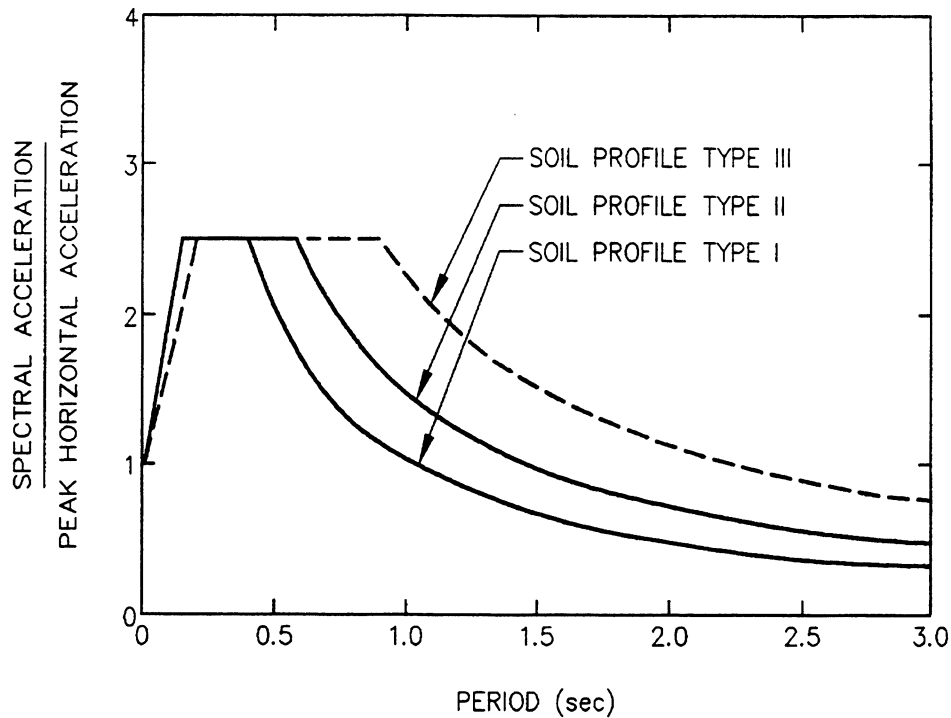


Figure 4-17: Normalized 1994 Uniform Building Code Response Spectra. (UBC, 1994, reproduced from the Uniform Building Code™, copyright© 1994, with the permission of the publisher, the International Conference of Building Officials)

The 1997 version of the UBC has six classes of site conditions and incorporates the effects of near-field ground motion. The six classes of site conditions incorporated in the 1997 UBC, designated S_A through S_F , are defined in Table 4-3 on the basis of the average shear wave velocity in the top 30 meters and other relevant geotechnical characteristics. The acceleration response spectra for classes S_A through S_E are based on Figure 4-18. For site class S_F , a site specific analysis is required to develop the response spectrum. The value of C_a , the spectral acceleration at zero period for the UBC spectra, is equal to the peak ground acceleration with a 10 percent probability of not being exceeded in 50 years. For site classes S_A through S_E , C_a may be taken from Table 4-4 in combination with the use of Figure 3-4 (to determine the Seismic Zone Factor, Z). For site class S_F , a site-specific analysis is required to evaluate C_a . The value of C_v for developing the UBC spectra described by Figure 4-18 is a function of the site class and UBC seismic zone factor (Figure 3-4 and Table 4-5).

For sites close to active faults (i.e. sites in zone 4), the Near Source Factors defined by Tables 4-6 through 4-8 should be applied to C_a and C_v . Vertical spectral accelerations are generally assumed equal to 2/3 of the horizontal spectral accelerations. However, for cases where a Near Source Factor greater than 1.0 is applied to the horizontal spectra, the UBC requires a site-specific analysis to develop the vertical response spectra.

While building code response spectra are useful to illustrate the effect of local soil conditions on ground response, these spectra represent effective spectral accelerations for use in structural design and are not intended to represent smoothed spectra from actual earthquakes. To represent an actual earthquake

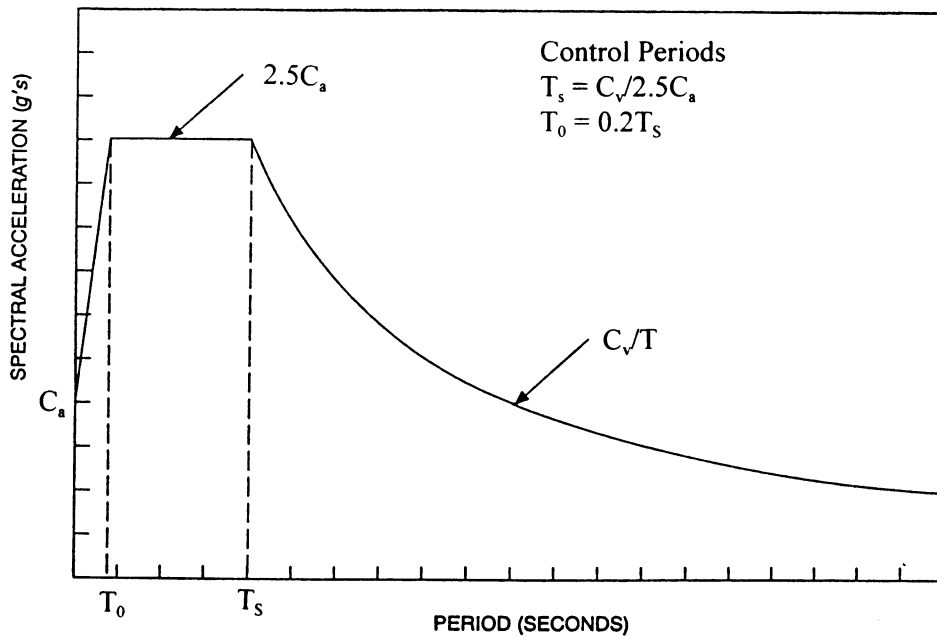


Figure 4-18: 1997 Uniform Building Code Design Response Spectra (UBC, 1997, reproduced from the Uniform Building Code™, copyright© 1997, with the permission of the publisher, the International Conference of Building Officials)

TABLE 4-3
1997 UBC SITE CLASSIFICATION

Designation	Site Class	Shear Wave Velocity ¹	Other Characteristics ²
S _A	Hard Rock	> 1500 m/s	
S _B	Rock	760 m/s to 1500 m/s	
S _C	Very Dense Soil and Soft Rock	360 m/s to 760 m/s	N > 50, S _u > 100 kPa
S _D	Stiff Soil	180 m/s to 360 m/s	15 < N < 50 50 kPa < S _u < 100 kPa
S _E	Soft Soil	Less than 180 m/s	More than 3m of soil with PI > 20, W _n > 40%, and S _u < 25 kPa
S _F	Special Soils		Collapsible, liquefiable, sensitive soils; More than 3m of peat or highly organic; More than 7.5m of clay with PI > 75; More than 36m of soft to medium clay.

- Notes: 1. Average shear wave velocity for upper 30m.
 2. N = standard Penetration Test Blow Count
 S_u = Undrained Shear Strength
 PI = Plasticity Index
 W_n = Moisture content

**TABLE 4-4
SEISMIC COEFFICIENT C_s**

Soil Profile Type	Seismic Zone Factor, Z				
	$Z = 0.075$	$Z = 0.15$	$Z = 0.2$	$Z = 0.3$	$Z = 0.4$
S_A	0.06	0.12	0.16	0.24	$0.32N_s$
S_B	0.08	0.15	0.20	0.30	$0.40N_s$
S_C	0.09	0.18	0.24	0.33	$0.40N_s$
S_D	0.12	0.22	0.28	0.36	$0.44N_s$
S_E	0.19	0.30	0.34	0.36	$0.36N_s$
S_F	See Footnote 1				

Notes: ¹ Site-specific geotechnical investigation and dynamic site response analysis shall be performed to determine seismic coefficients for Soil Profile Type S_F .

**TABLE 4-5
SEISMIC COEFFICIENT C_v**

Soil Profile Type	Seismic Zone Factor, Z				
	$Z = 0.075$	$Z = 0.15$	$Z = 0.2$	$Z = 0.3$	$Z = 0.4$
S_A	0.06	0.12	0.16	0.24	$0.32N_v$
S_B	0.08	0.15	0.20	0.30	$0.40N_v$
S_C	0.13	0.25	0.32	0.45	$0.56N_v$
S_D	0.18	0.32	0.40	0.54	$0.64N_v$
S_E	0.26	0.50	0.64	0.84	$0.96N_v$
S_F	See Footnote 1				

Notes: ¹ Site-specific geotechnical investigation and dynamic site response analysis shall be performed to determine seismic coefficients for Soil Profile Type S_F .

**TABLE 4-6
SEISMIC SOURCE TYPE¹**

Seismic Source Type	Seismic Source Description	Seismic Source Definition ²	
		Max. Moment Magnitude, M	Slip Rate, SR (mm/yr)
A	Faults that are capable of producing large magnitude events and that have a high rate of seismic activity	$M \geq 7.0$	$SR \geq 5$
B	All faults other than types A and C	$M \geq 7.0$ $M < 7.0$ $M \geq 6.5$	$SR < 5$ $SR > 2$ $SR < 2$
C	Faults that are not capable of producing large magnitude earthquakes and that have a relatively low rate of seismic activity	$M < 6.5$	$SR \leq 2$

Notes: ¹ Subduction sources shall be evaluated on a site-specific basis.

² Both maximum moment magnitude and slip rate conditions must be satisfied concurrently when determining the seismic source type.

**TABLE 4-7
NEAR-SOURCE FACTOR N_s ¹**

Seismic Source Type	Closest Distance to Known Seismic Source ^{2,3}		
	≤ 2 km	5 km	≥ 10 km
A	1.5	1.2	1.0
B	1.3	1.0	1.0
C	1.0	1.0	1.0

Notes: ¹ The Near-Source Factor may be based on the linear interpolation of values for distances other than those show in the table.
² The location and type of seismic sources to be used for design shall be established based on approved geotechnical data.
³ The closest distance to seismic source shall be taken as the minimum distance between the site and the area described by the vertical projection of the source on the surface. The surface projection need not include portions of the source depths of 10 km or greater. The largest value of the Near-Source Factor considering all sources shall be used for design.

**TABLE 4-8
NEAR-SOURCE FACTOR N_v ¹**

Seismic Source Type	Closest Distance to Known Seismic Source ^{2,3}			
	≤ 2 km	5 km	10 km	≥ 15 km
A	2.0	1.6	1.2	1.0
B	1.6	1.2	1.0	1.0
C	1.0	1.0	1.0	1.0

Notes: ¹ The Near-Source Factor may be based on the linear interpolation of values for distances other than those show in the table.
² The location and type of seismic sources to be used for design shall be established based on approved geotechnical data.
³ The closest distance to seismic source shall be taken as the minimum distance between the site and the area described by the vertical projection of the source on the surface. The surface projection need not include portions of the source depths of 10 km or greater. The largest value of the Near-Source Factor considering all sources shall be used for design.

spectrum, the spectrum generated from an attenuation relationship, or the spectrum from seismic site response analysis (see Chapter 6) should be used.

In May 1997, FHWA and the National Center for Earthquake Engineering Research (NCEER) jointly sponsored a workshop on the “National Representation of Seismic Ground Motion for New and Existing Highway Facilities” (Friedland, et. Al, 1997). Among the issues considered at the workshop were:

- Should the USGS maps and UBC code provisions be used for highway facilities;
- Should vertical and near-source ground motions be specified for design; and
- Should spatial variations of ground motions be specified for design?

While building code response spectra are useful to illustrate the effect of local soil conditions on ground Workshop participants concluded that, while the 1996 USGS maps provide the basis for a national portrayal of seismic hazard for highway facilities, design of highway facilities to prevent collapse should consider design ground motions at probabilities lower than 10 percent probability of exceedence in 50 years that is currently in AASHTO and the UBC. The workshop participants recommended to develop seismic hazard maps for highway facilities similar to the 1997 National Earthquake Hazard Reduction Program (NEHRP) provisions for collapse- prevention design of building, wherein the USGS maps for 2% probability of exceedence in 50 years truncated by deterministic peak values in areas of high seismicity was recommended.

Workshop participants concluded that the 1997 UBC spectra, with separate sets of short and long period factors dependant on the intensity of ground shaking, with increased amplification for low levels of shaking, and 1/T decay at long periods, were more appropriate than the current AASHTO provisions for highway facilities design.

Workshop participants also concluded that because the high vertical motions in near-source regions can significantly impact bridge response, vertical ground motions should be specified for certain types of bridges in higher seismic zones. Furthermore, because near-source motions have certain unique characteristics not captured in current UBC or NEHRP spectral shapes, new approaches to specifying near field motions are needed. Workshop participants also recognized that the response of “ordinary” highway bridges is not greatly affected by spatial variations of ground motion, but that spatial variations can be important in some cases and that research is needed to define and address these cases.

4.6.3 Energy and Duration

Local soil conditions can also affect duration and energy content. Energy and durations on soil sites have greater scatter and tend to be longer than durations on rock sites. In fact, the range of energy and durations for rock sites appears to be a lower bound for soil site durations. The FHWA/NCEER workshop participants concluded that energy is a more fundamental parameter, influencing structural response. However, no accepted energy-based design procedures are currently available. For some geotechnical problems, duration may be as important as energy content.

4.6.4 Resonant Site Frequency

Amplification of long period bedrock motions by local soil deposits and constructed dams/embankments and soil retaining systems is now accepted as an important phenomenon that can exert a significant influence on the damage potential of earthquake ground motions. Significant structural damage has been attributed to amplification of both peak acceleration and spectral acceleration by local soil conditions. Amplification of peak acceleration occurs when the resonant frequency of the soil deposits or soil structure is close to the predominant frequencies of the bedrock earthquake motions (the frequencies associated with the peaks of the acceleration response spectra). The *resonant frequency*, f_o , of a horizontal soil layer (deposit) of thickness H can be estimated as a function of the average shear wave velocity of the layer, $(V_s)_{avg}$, using the following equation:

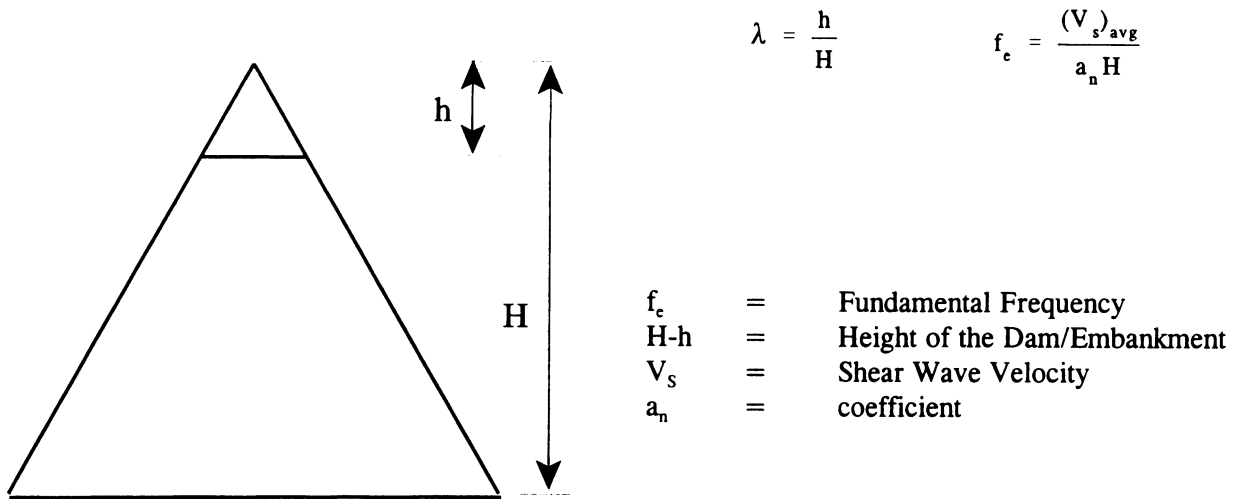
$$f_o = \frac{(V_s)_{avg}}{4H} \quad (4-5)$$

The resonant frequency of a trapezoidal embankment, f_c , can be estimated using a similar equation of the form:

$$f_c = \frac{(V_s)_{avg}}{a_n H} \quad (4-6)$$

where the coefficient a_n varies between 2.4 and 4 as shown in Figure 4-19.

Amplification of the spectral acceleration may occur at soil sites in any earthquake at frequencies around the resonant frequency of the soil deposit. Some of the most significant damage in recent earthquakes



λ	a_n
0.00	2.405
0.03	2.409
0.05	2.416
0.10	2.448
0.15	2.501
0.20	2.574
0.25	2.668
0.30	2.786
0.35	2.930
0.40	3.107
0.45	3.323
0.50	3.588
1.00	4.0

Note: For $0.5 \leq \lambda \leq 1.0$, a_n may be derived by linear interpolation from $a_n = 3.6$ for $\lambda = 0.5$ to $a_n = 4.0$ for $\lambda = 1.0$.

Figure 4-19: Fundamental Frequency of Trapezoidal Dam/Embankment

(e.g., building damage in Mexico City in the 1985 earthquake and damage to freeway structures in the Loma Prieta earthquake of 1989) has occurred in situations where the predominant frequencies of the bedrock motions and the resonant frequencies of both the local soil deposit and the overlying structure all fell within the same range.

4.7 SELECTION OF REPRESENTATIVE TIME HISTORIES

Earthquake time histories may be required for input to both seismic site response analyses (see Chapter 6) and seismic deformation analyses (see Chapter 7). There are several procedures that can be used to select earthquake ground motions at a site. These procedures include:

- selection of motions previously recorded for similar site conditions during a similar earthquake and at distances comparable to those under consideration;
- selection of generic, publicly available synthetic ground motions generated to represent an event of the target magnitude;
- estimation of a *target spectrum* (a spectrum representative of the design magnitude, site-to-source distance, and local geology (soil or rock) using either an attenuation relationship or a code or standard) and then selection of recorded or synthetic time histories whose special ordinates are either comparable to or envelope those of the target spectrum for the period range of interest; or
- use of simulation techniques to generate a project-specific synthetic time history, starting from the source and propagating the appropriate wave forms to the site to generate a suite of time histories that can then be used to represent the earthquake ground motions at the site of interest.

In selecting a representative time history from the catalog of available records, an attempt should be made to match as many of the relevant characteristics of the design earthquake as possible. Important characteristics that should be considered in selecting a time history include:

- earthquake magnitude;
- source mechanism (e.g., strike slip, dip slip, or oblique faulting);
- focal depth;
- site-to-source distance;
- site geology;
- peak ground acceleration;
- frequency content;
- duration; and
- energy content (RMSA or I_A).

The relative importance of these factors varies from case to case. For instance, if a bedrock record is chosen for use in a site response analysis to model the influence of local soil conditions, site geology will not be particularly important in selection of the input bedrock time history. However, if a soil site record is to be scaled to a specified peak ground acceleration, site geology can be a critical factor in selection of an appropriate time history, as the record must already include any potential influence of local soil conditions on the motion. Scaling of the peak acceleration of a strong motion record by a factor of more than two is not recommended, as the frequency characteristics of ground motions can be directly and indirectly related to the amplitude of the motion. Leeds (1992) and Naeim and Anderson (1993) present comprehensive databases of available strong motion records and their characteristics. These strong motion

records can be obtained in digital form (CD-ROM) from the National Geophysical Data Center (NGDC) in Boulder, Colorado. Also, Tao (1996) provides detailed information on several other sources from which accelerograms can be obtained directly via on-line systems or purchased in a variety of formats.

Due to uncertainties in the selection of a representative earthquake time history, response analyses are usually performed using a suite of time histories rather than a single time history. Engineers commonly use two to five time histories to represent each significant seismic source in a site response analysis. The 1997 UBC requires a minimum of three pairs of time histories from recorded events for time history analysis. For earthquakes in the western United States, it should be possible to find three to five representative time histories that satisfy the above criteria. However, at the present time, there are a limited number of bedrock strong motion records available from earthquakes of magnitude M_w 5.0 or greater in the central and eastern United States or Canada, including:

- eight records from the 1988 Saguenay, Quebec earthquake of magnitude M_w 5.9;
- three records from the 1985 Nahanni; Northwest Territories (Canada) Earthquake of Magnitude M_w 6.7; and
- the Loggie Lodge record with a peak horizontal acceleration of 0.4 g from the 1981 Mirimichi, New Brunswick earthquake of magnitude M_w 5.0.

Therefore, for analysis of sites east of the Rocky Mountains, records from a western United States site, an international recording site or synthetic accelerograms are often used to compile a suite of at least three records for analysis.

Generic, synthetically generated ground motions are available only for a limited number of major faults (fault systems). For example, Jennings, *et al.* (1968) developed the A1 synthetic accelerogram for soil site conditions for an earthquake on the southern segment of the San Andreas fault. Seed and Idriss (1969) developed a synthetic accelerogram for rock sites for an earthquake on the northern segment of the San Andreas fault. The Jennings, *et al.* (1968) A1 accelerogram has an energy content which is larger than the energy content of any accelerogram recorded to date. For this reason, the A1 record is often used to simulate major earthquakes in the Cascadia and New Madrid seismic zones. Appropriate synthetic accelerograms may also be available to the engineer from previous studies and may be used if they are shown to be appropriate for the site. Synthetic earthquake accelerograms for many regions of the country are currently being compiled by the Lamont-Doherty Earth Observatory of Columbia University under the auspices of the Multi-Disciplinary Center for Earthquake Engineering Research (formally National Center for Earthquake Engineering Research, NCEER) and can be downloaded from the NCEER website at "<http://nceer.eng.buffalo.edu>. A catalog of records representative on northeastern United States seismicity (i.e., Boston) was recently developed for a Federal Emergency Management Agency (FEMA) research project on the performance of steel buildings (Somerville, *et al.*, 1998). These records can be downloaded from the Earthquake Engineering Research Center (EERC) website at "http://quiver.eerc.berkeley.edu:8080/studies/system/ground_motions.html."

The *target spectrum* may be estimated from available attenuation relationships (see Section 4.3). These attenuation relationships, typically developed for a spectral damping of 5 percent, provide estimates of the median spectral ordinates and the log-normal standard deviation about the mean. Representative time histories are selected by trial-and-error on the basis of "reasonable" match with the target spectrum. A "reasonable" match does not necessarily mean that the response spectrum for the candidate record "hugs" the target spectrum. Particularly if a suite of time histories is used, a "reasonable" match only requires that the suite of response spectra averaged together approximates the mean target spectrum. Each individual spectrum may fluctuate within the plus and minus one standard deviation bounds over most of

the period range of interest. Natural and/or generic synthetic time histories can be screened in this type of selection process.

An alternative approach to trial-and-error matching of the target spectrum is computerized generation of a synthetic time history or a suite of time histories whose spectral ordinates provide a reasonable envelope to those of the target spectrum. Existing time histories can also be modified to be spectrum compatible. Several computer programs are available for these tasks (e.g., Gasparin and Vanmarcke, 1976; Ruiz and Penzien, 1969; Silva and Lee, 1987). However, generation of realistic synthetic ground motions is not within the technical expertise of most geotechnical engineering consultants. The simulation programs should only be used by qualified engineering seismologists and earthquake engineers. For this reason, these simulation techniques are beyond the scope of this guidance document.

CHAPTER 8.0 LIQUEFACTION AND SEISMIC SETTLEMENT

8.1 INTRODUCTION

During strong earthquake shaking, loose, saturated cohesionless soil deposits may experience a sudden loss of strength and stiffness, sometimes resulting in loss of bearing capacity, large permanent lateral displacements, and/or seismic settlement of the ground. This phenomenon is called *soil liquefaction*. In the absence of saturated or near-saturation conditions, strong earthquake shaking can induce compaction and settlement of the ground. This phenomenon is called *seismic settlement*.

Liquefaction and/or seismic settlement beneath and in the vicinity of highway facilities can have severe consequences with respect to facility integrity. Localized bearing capacity failures, lateral spreading, and excessive settlements resulting from liquefaction may damage bridges, embankments, and other highway structures. Liquefaction-associated lateral spreading and flow failures and seismically-induced settlement can also affect the overall stability of the roadway. Similarly, excessive total or differential settlement can impact the integrity and/or serviceability of highway facilities. Therefore, a liquefaction and seismic settlement potential assessment is a key element in the seismic design of highways.

This Section outlines the current state-of-the-practice for evaluation of the potential for, and the consequences of (should it occur), soil liquefaction and seismic settlement as they apply to the seismic design of highways. Initial screening criteria to determine whether or not a liquefaction analysis is needed for a particular project are presented in Section 8.2. The simplified procedure for liquefaction potential assessment commonly used in engineering practice is presented in Section 8.3. Methods for performing a liquefaction impact assessment, i.e., to estimate post-liquefaction deformation and stability, are presented in Section 8.4. The simplified procedures for seismic settlement of unsaturated sand evaluation commonly used in engineering practice are presented in Section 8.5. Methods for mitigation of liquefaction and seismic settlement potential and of the consequences of liquefaction are discussed in Section 8.6. Advanced methods for liquefaction potential assessments, including one- and two-dimensional fully-coupled effective stress site response analyses, are briefly discussed in Section 8.3.

8.2 FACTORS AFFECTING LIQUEFACTION SUSCEPTIBILITY

The first step in any liquefaction evaluation is to assess whether the potential for liquefaction exists at the site. A variety of screening techniques exist to distinguish sites that are clearly safe with respect to liquefaction from those sites that require more detailed study (e.g., Dobry, *et al.*, 1980). The following five screening criteria are most commonly used to make this assessment:

- *Geologic age and origin.* Liquefaction potential decreases with increasing age of a soil deposit. Pre-Holocene age soil deposits generally do not liquefy, though liquefaction has occasionally been observed in Pleistocene-age deposits. Table 8-1 presents the liquefaction susceptibility of soil deposits as a function of age and origin (Youd and Perkins, 1978).
- *Fines content and plasticity index.* Liquefaction potential decreases with increasing fines content and increasing plasticity index, PI. Data presented in Figure 8-1 (Ishihara, *et al.*, 1989) show grain size distribution curves of soils known to have liquefied in the past. This data serves as a rough guide for liquefaction potential assessment of cohesionless soils. Soils having greater than 15 percent (by

TABLE 8-1
SUSCEPTIBILITY OF SEDIMENTARY DEPOSITS
TO LIQUEFACTION DURING STRONG SHAKING
 (After Youd and Perkins, 1978, Reprinted by Permission of ASCE)

Type of Deposit	General Distribution of Cohesionless Sediments in Deposits	Likelihood that Cohesionless Sediments, When Saturated, Would Be Susceptible to Liquefaction (by Age of Deposit)			
		< 500 Year	Holocene	Pleistocene	Pre-pleistocene
Continental Deposits					
River channel	Locally variable	Very high	High	Low	Very low
Flood plain	Locally variable	High	Moderate	Low	Very low
Alluvial fan and plain	Widespread	Moderate	Low	Low	Very low
Marine terraces and plains	Widespread	—	Low	Very low	Very low
Delta and fan-delta	Widespread	High	Moderate	Low	Very low
Lacustrine and playa	Variable	High	Moderate	Low	Very low
Colluvium	Variable	High	Moderate	Low	Very low
Talus	Widespread	Low	Low	Very low	Very low
Dunes	Widespread	High	Moderate	Low	Very low
Loess	Variable	High	High	High	Unknown
Glacial till	Variable	Low	Low	Very low	Very low
Tuff	Rare	Low	Low	Very low	Very low
Tephra	Widespread	High	High	Unknown	Unknown
Residual soils	Rare	Low	Low	Very low	Very low
Sebka	Locally variable	High	Moderate	Low	Very low
Coastal Zone					
Delta	Widespread	Very high	High	Low	Very low
Esturine	Locally variable	High	Moderate	Low	Very low
Beach-high wave energy	Widespread	Moderate	Low	Very low	Very low
Beach-low wave energy	Widespread	High	Moderate	Low	Very low
Lagoonal	Locally variable	High	Moderate	Low	Very low
Fore shore	Locally variable	High	Moderate	Low	Very low
Artificial Deposits					
Uncompacted fill	Variable	Very high	—	—	—
Compacted fill	Variable	Low	—	—	—

weight) finer than 0.005 mm, a liquid limit greater than 35 percent, or an in-situ water content less than 0.9 times the liquid limit generally do not liquefy (Seed and Idriss, 1982).

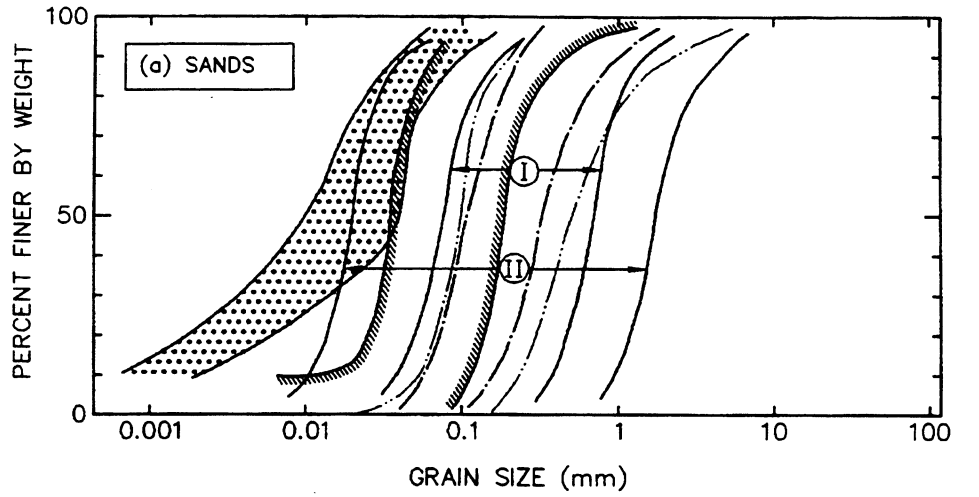
- *Saturation.* Although unsaturated soils have been reported to liquefy, at least 80 to 85 percent saturation is generally deemed to be a necessary condition for soil liquefaction. In many locations, the water table is subject to seasonal oscillation. In general, it is prudent that the highest anticipated seasonal water table elevation be considered for initial screening.
- *Depth below ground surface.* While failures due to liquefaction of end-bearing piles resting on sand layers up to 30 m below the ground surface have been reported, shallow foundations are generally not affected if liquefaction occurs more than 15 m below the ground surface.
- *Soil penetration resistance.* According to the data presented in Seed and Idriss (1982), liquefaction has not been observed in soil deposits having normalized Standard Penetration Test (SPT) blow counts, $(N_1)_{60}$ larger than 22. Marcuson, *et al.* (1990) suggest a normalized SPT value of 30 as the threshold value above which liquefaction will not occur. However, Chinese experience, as quoted in Seed, *et al.* (1983), suggests that in extreme conditions liquefaction is possible in soils having normalized SPT blow counts as high as 40. Shibata and Teparaska (1988), based on a large number of observations, conclude that no liquefaction is possible if normalized Cone Penetration Test (CPT) cone resistance, q_{cl} , is larger than 15 MPa.

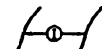
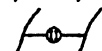


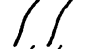
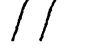
If three or more of the above criteria indicate that liquefaction is *not* likely, the potential for liquefaction may be considered to be small enough that a formal liquefaction potential analysis is not required. If, however, based on the above initial screening criteria, the potential for liquefaction of a cohesionless soil layer beneath the site cannot be dismissed, more rigorous analysis of liquefaction potential is needed.

Liquefaction susceptibility maps, derived on the basis of some (or all) of the above listed criteria, are available for many major urban areas in seismic zones (e.g., Kavazanjian, *et al.*, 1985b for San Francisco; Tinsley, *et al.*, 1985 for Los Angeles; Hadj-Hamou and Elton, 1988 for Charleston, South Carolina; Hwang and Lee, 1992 for Memphis). These maps may be useful for preliminary screening analyses for highway routing studies. However, as most new highways are sited outside major urban areas, these types of maps are unlikely to be available for many highway sites. Furthermore, most of these maps do not provide sufficient detail to be useful for site-specific studies or detailed design analyses.

Several attempts have been made to establish threshold criteria for values of seismic shaking that can induce liquefaction (e.g., minimum earthquake magnitude, minimum peak horizontal acceleration, maximum distance from causative fault). Most of these criteria have eventually been shown to be misleading, since even low intensity bedrock ground motions from distant earthquakes can be amplified by local soils to intensity levels strong enough to induce liquefaction, as observations of liquefaction in the 1985 Mexico City and 1989 Loma Prieta earthquakes demonstrate.

Most soil deposits known to have liquefied are sand deposits. However, as indicated on Figure 8-1, some deposits containing gravel particles (> 2 mm size) in a fine grained soil matrix may be susceptible to liquefaction. Discussion of the liquefaction potential of gravel deposits is beyond the scope of this document. The reader is referred to Ishihara (1985), Harder (1988), and Stark and Olson (1995) for a discussion of methods for evaluation of the liquefaction potential of gravels.



-  : BOUNDARY FOR MOST LIQUEFIABLE SOIL
 -  : BOUNDARY FOR POTENTIALLY LIQUEFIABLE SOIL
 -  : TAILINGS SLIME (ISHIHARA, 1985)
 -  : LIQUEFIED SAND IN CHIBA-TOHO-OKI EQ. (1987)
 -  : LIQUEFIED SAND IN NIIGATA EQ.(1964)
 -  : LIQUEFIED SAND IN NIHONKAI-CHUBU EQ. (1983)
- } (TSUCHIDA, 1970)

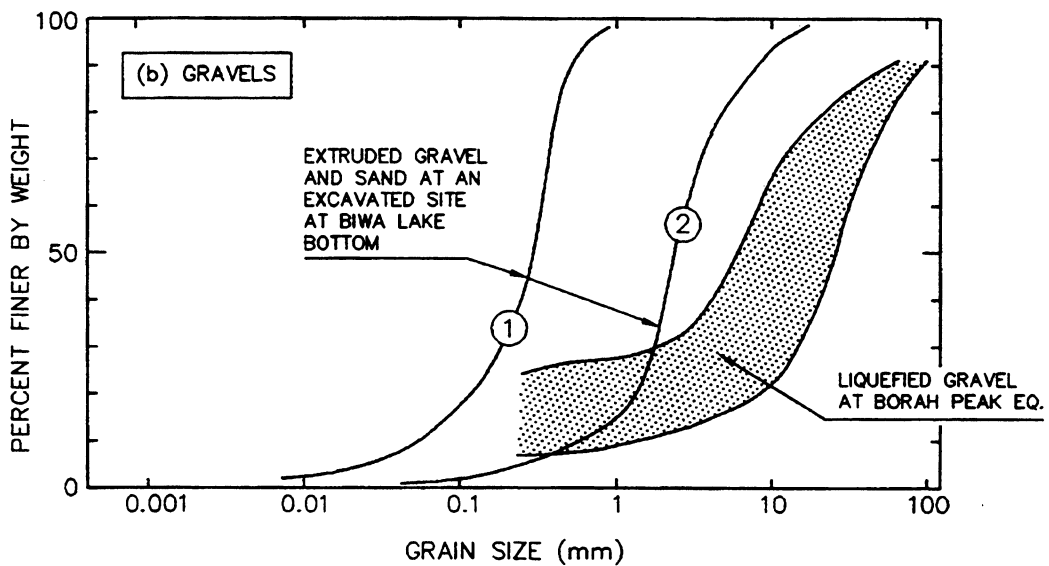


Figure 8-1: Grain Size Distribution Curves of Potentially Liquefiable Soils. (Modified after Ishihara, *et al.*, 1989, reprinted with permission of A.A. Balkema, Old Post Rd., Brookfield, VT 05036)

8.3 EVALUATION OF LIQUEFACTION POTENTIAL

8.3.1 Introduction

Due to the difficulties in obtaining and testing undisturbed representative samples from most potentially liquefiable soil materials, in situ testing is the approach preferred by most engineers for evaluating the liquefaction potential of a soil deposit. Liquefaction potential assessment procedures involving both the SPT and CPT are widely used in practice (e.g., Seed and Idriss, 1982; Ishihara, 1985; Seed and De Alba, 1986; Shibata and Teparaska, 1988; Stark and Olson, 1995). For gravelly soils, the Becker Penetration Test (BPT) is commonly used to evaluate liquefaction potential (Harder and Seed, 1986). Geophysical techniques for measuring shear wave velocity have recently emerged as potential alternatives for liquefaction potential assessment (Tokimatsu, *et al.*, 1991; Youd and Idriss, 1997).

8.3.2 Simplified Procedure

The most common procedure used in engineering practice for the liquefaction potential assessment of sands and silts is the *Simplified Procedure* originally developed by Seed and Idriss (1982). Since its original development, the original Simplified Procedure as proposed by Seed and Idriss has been progressively revised, extended, and refined (Seed, *et al.*, 1983; Seed, *et al.*, 1985; Seed and De Alba, 1986; Liao and Whitman, 1986). The Simplified Procedure may be used with either SPT or CPT data. Recent summaries of the various revisions to the Simplified Procedure are provided by Marcuson, *et al.*, (1990) and Seed and Harder (1990). A 1996 workshop sponsored by the National Center for Earthquake Engineering Research (NCEER) reviewed recent developments on evaluation of liquefaction resistance of soils and arrived consensus on improvements and augmentation to the simplified procedure (Youd and Idriss, 1997). Based primarily on recommendations from these studies, the Simplified Procedure for evaluating liquefaction potential at the site of highway facilities can be performed using the following steps:

- Step 1: From borings and soundings, in situ testing and laboratory index tests, develop a detailed understanding of the project site subsurface conditions, including stratigraphy, layer geometry, material properties and their variability, and the areal extent of potential problem zones. Establish the zones to be analyzed and develop idealized, representative sections amenable to analysis. The subsurface data used to develop the representative sections should include the location of the water table, either SPT blow count, N , or tip resistance of a standard CPT cone, q_c , mean grain size, D_{50} , unit weight, and the percentage of fines in the soil (percent by weight passing the U.S. Standard No. 200 sieve).
- Step 2: Evaluate the total vertical stress, σ_v , and effective vertical stress, σ_v' , for all potentially liquefiable layers within the deposit both at the time of exploration and for design. Vertical and shear stress design values should include the stresses resulting from facility construction. Exploration and design values for vertical total and effective stress may be the same or may differ due to seasonal fluctuations in the water table or changes in local hydrology resulting from project development. Note that for underwater sites, the total weight of water above the mudline should not be included in calculating the total vertical stress. Also evaluate the initial static shear stress on the horizontal plane, τ_{ho} , for design.
- Step 3: If results of a site response analysis are not available, evaluate the *stress reduction factor*, r_d as described below. The stress reduction factor is a soil flexibility factor defined as the ratio of the peak shear stress for the soil column, $(\tau_{max})_d$, to that of a rigid body, $(\tau_{max})_r$. There are several ways to obtain r_d . For non-critical projects, the following equations for r_d were recommended by

a panel of experts convened by the National Center for Earthquake Engineering Research (NCEER) in 1996 (Youd and Idriss, 1997):

$$\begin{aligned}
 r_d &= 1.0 - 0.00765 z && \text{for } z \leq 9.15 \text{ m} \\
 r_d &= 1.174 - 0.0267 z && \text{for } 9.15 \text{ m} < z \leq 23 \text{ m} \\
 r_d &= 0.744 - 0.008 z && \text{for } 23 < z \leq 30 \text{ m} \\
 r_d &= 0.5 && \text{for } z > 30 \text{ m}
 \end{aligned}
 \tag{8-1}$$

where z is the depth below the ground surface in meters. Mean values of r_d calculated from Equation 8-1 are plotted in Figure 8-2 along with the range of data proposed by Seed and Idriss (1971).

For critical projects warranting a site-specific response analysis, or if results of a site response analysis (see Chapter 6) are available, the maximum earthquake-induced shear stress at depth z , τ_{\max} , can be directly obtained from the results of the site response analysis. In this case, it may be convenient to calculate r_d from the site response results for use in spreadsheet calculations using the following equation:

$$r_d = \frac{(\tau_{\max})_{@depth=z}}{(\sigma_v)_{@depth=z} \cdot (a_{\max}/g)_{@surface}}
 \tag{8-2}$$

where σ_v is the total shear stress at depth z , a_{\max} is the peak ground surface acceleration, and g is the acceleration of gravity. The parameters σ_v and a_{\max} are also directly calculated by most site response computer programs described in Chapter 6.

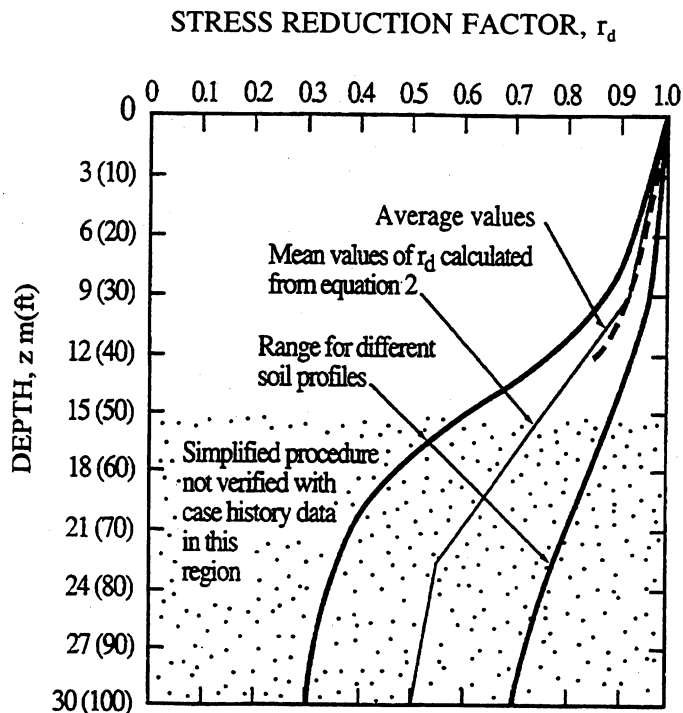


Figure 8-2: Stress Reduction Factor, r_d , Versus Depth Curves Developed by Seed and Idriss (1971) with Added Mean Value Lines from Equation 8-1.

Use of τ_{\max} from site response analysis (or use of the results of a site response analysis to evaluate r_d) is considered to be generally more reliable than any of the simplified approaches to estimate r_d , and is strongly recommended for sites that are marginal with respect to liquefaction potential (i.e., sites where the factor of safety for liquefaction is close to 1.0).

Step 4: Calculate the *critical stress ratio induced by the design earthquake*, CSR_{EQ} , as:

$$CSR_{EQ} = 0.65 (a_{\max}/g) r_d (\sigma_v/\sigma_v') \quad (8-3a)$$

If the results of a seismic site response analysis are available, CSR_{EQ} can be evaluated from τ_{\max} as:

$$CSR_{EQ} = 0.65 \tau_{\max}/\sigma_v' \quad (8-3b)$$

Note that the ratio τ_{\max}/σ_v' corresponds to the peak average acceleration denoted by k_{\max} in Chapter 6.

Step 5: Evaluate the *standardized SPT blow count*, N_{60} , using the procedure presented in Chapter 5.

Step 6: Calculate the normalized and standardized SPT blow count, $(N_1)_{60}$, using the procedure presented in Chapter 5

Step 7: Evaluate the critical stress ratio $CSR_{7.5}$ at which liquefaction is expected to occur during an earthquake of magnitude $M_w = 7.5$ as a function of $(N_1)_{60}$. Use the chart developed by Seed, *et al.* (1985) as modified by NCEER, shown in Figure 8-3, to find $CSR_{7.5}$. It should be noted that this chart was developed using a large database from sites where liquefaction did or did not occur during past earthquakes. The general conditions for the case history data presented in this chart are as follows: (1) all sites evaluated were under level ground condition, (2) the effective overburden pressure for all cases does not exceed 96 kPa, and (3) the magnitude of the earthquakes considered in all cases was in the neighborhood of 7.5.

Step 8: Calculate the *corrected critical stress ratio resisting liquefaction*, CSR_L . CSR_L is calculated as:

$$CSR_L = CSR_{7.5} \cdot k_M \cdot k_\sigma \cdot k_\alpha \quad (8-4)$$

where k_M is the correction factor for earthquake magnitudes other than 7.5, k_σ is the correction factor for stress levels larger than 96 kPa, and k_α is the correction factor for the initial driving static shear stress, τ_{ho} . Previous investigators have derived various recommendations on the magnitude correction factor, K_M , as shown in Figure 8-4. Upon review of all the data, the NCEER workshop participants have recommended a range of K_M values for design and analysis purposes. Their recommendations are presented in Figure 8-4. For effective confining pressures σ'_m larger than 96 kPa, k_σ can be determined from Figure 8-5 (Youd and Idriss, 1997). For σ'_m less than or equal to 96 kPa, no correction is required.

The value of k_α depends on both τ_{ho} and the relative density of the soil, D_r . On sloping ground, or below structures and embankments, τ_{ho} can be estimated using various closed-form elastic solutions (e.g., Poulos and Davis, 1974) or using the results of finite element (static) analyses. Once τ_{ho} and σ_v' are estimated, k_α can be determined from Figure 8-6, originally proposed by Seed

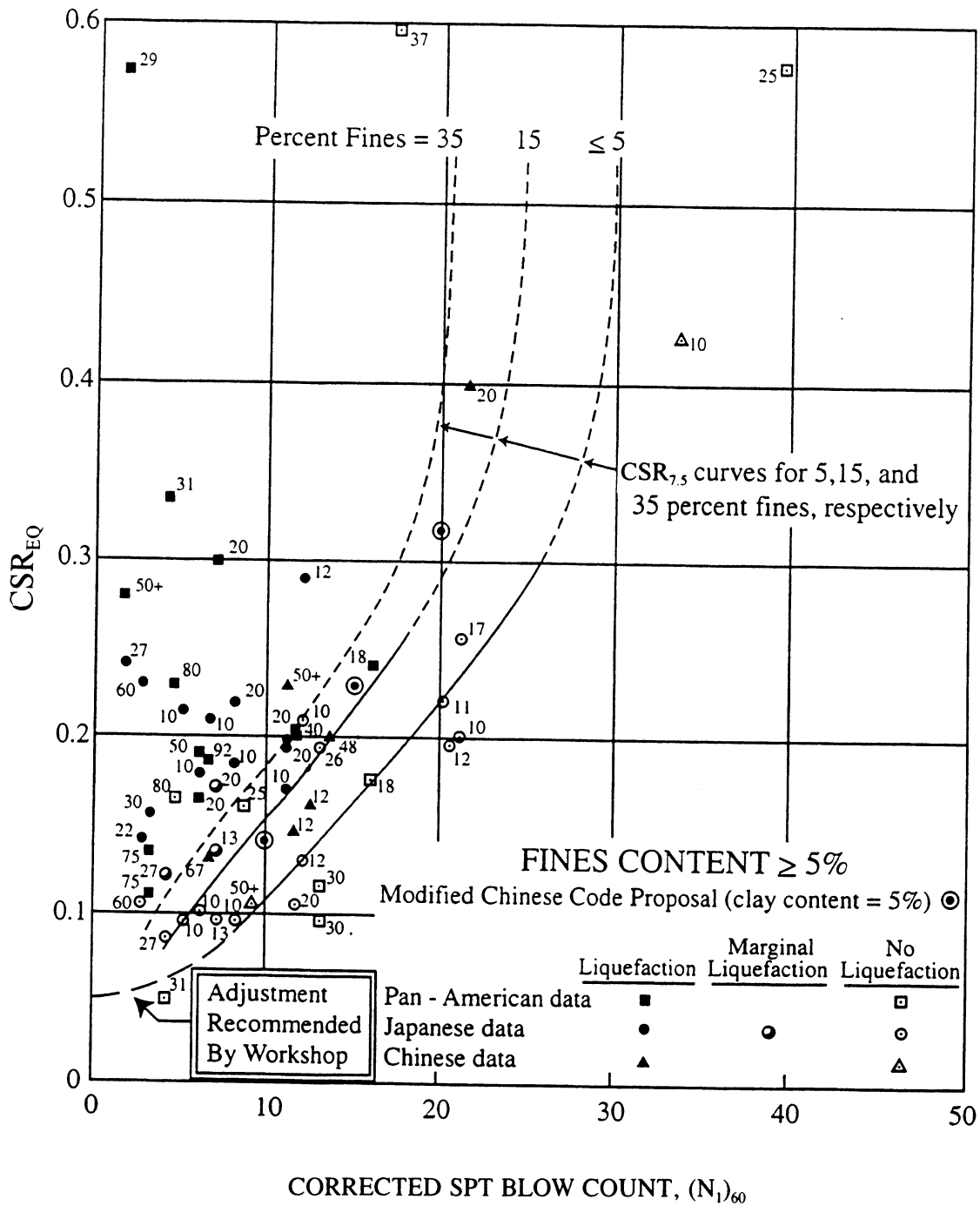


Figure 8-3: Relationship Between Cyclic Stress Ratio Causing Liquefaction and SPT (N₁)₆₀ Values for Sands for M = 7.5 Earthquakes (modified From Seed et al., 1985)

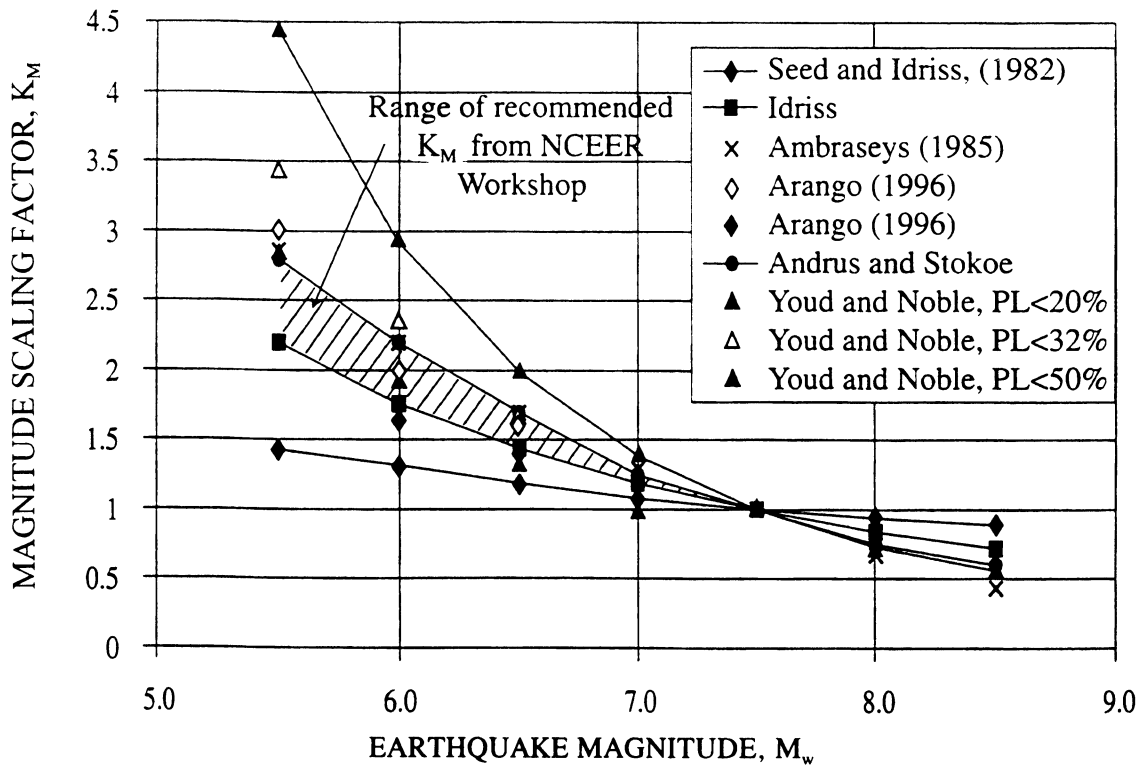


Figure 8-4: Magnitude Scaling Factors Derived by Various Investigators (After Youd and Idriss, 1997)

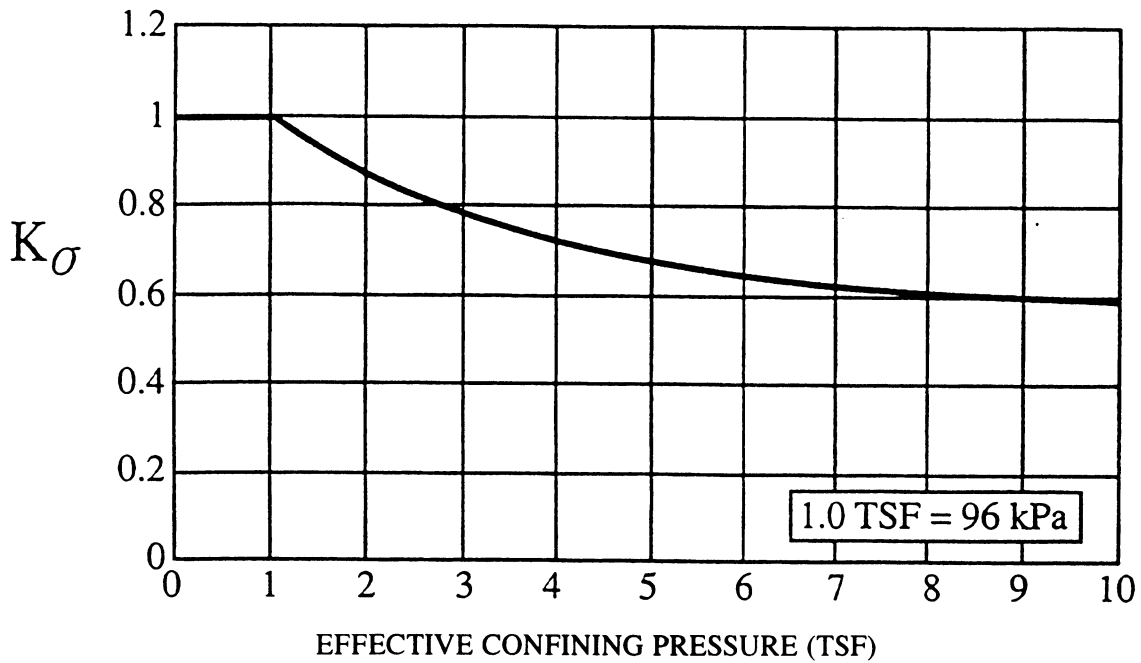


Figure 8-5: Recommended Correction Factor k_σ . (After Youd and Idriss, 1997)

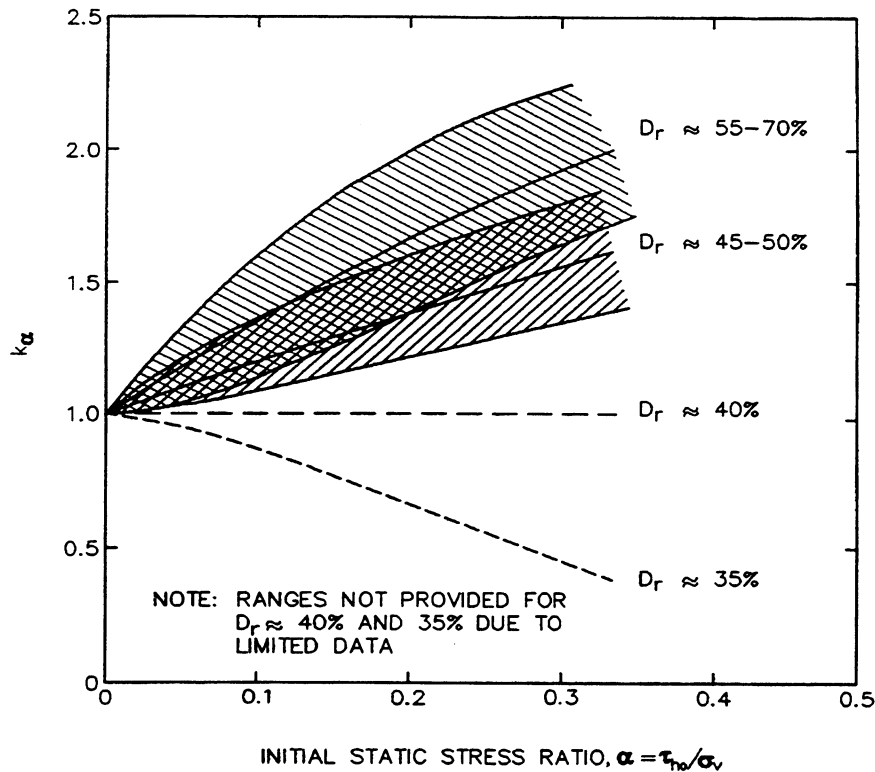


Figure 8-6: Curves for Estimation of Correction Factor, k_α . (Harder, 1988 and Hynes, 1988, as cited in Marcuson, *et al.*, 1990, reprinted by permission of EERI)

(1983) and modified by Harder (1988) and Hynes (1988). However, experts participating in the 1996 NCEER workshop on "Evaluation of Liquefaction Resistance of Soils" (1997) have concluded that due to the wide range of k_α values developed from previous studies and a lack of consistency of the results, general recommendations for use of k_α for design purposes are not advisable at this time. The evaluation of liquefaction resistance beneath sloping ground or embankments is not well understood and further research is required.

The effect of plasticity index on liquefaction resistance has also been reported (Ishihara, 1990). It is generally recognized that liquefaction resistance increases with soil plasticity. For example, many practitioners have been applying a 10 percent increase to the liquefaction resistance for soils with a plasticity index greater than 15 percent. However, a reliable correction relationship could not be formulated at this time due to the lack of data (Youd and Idriss, 1997).

Liquefaction resistance based on SPT (or CPT) measurements could not be reliably estimated for gravelly soils. Large gravel particles tend to increase the penetration resistance of the penetrometer unproportionately. To overcome this difficulty, large-diameter penetrometers have been used by some investigators. The Becker penetration test (BPT) has become the more effective and most widely used of this type of tools. There are correlations between Becker blowcount and SPT blowcount. The correlation proposed by Harder (1997) is recommended for liquefaction evaluation of gravelly soils in cases where Becker penetration testing data are available. Detailed information on the procedure is presented in the NCEER report (Youd and Idriss, 1997). In the absence of Becker penetration testing data, the effects of gravel content can be roughly estimated using the correlation curve shown in Figure 8-7 (Ishihara, 1985). The "Cyclic Strength of Sand

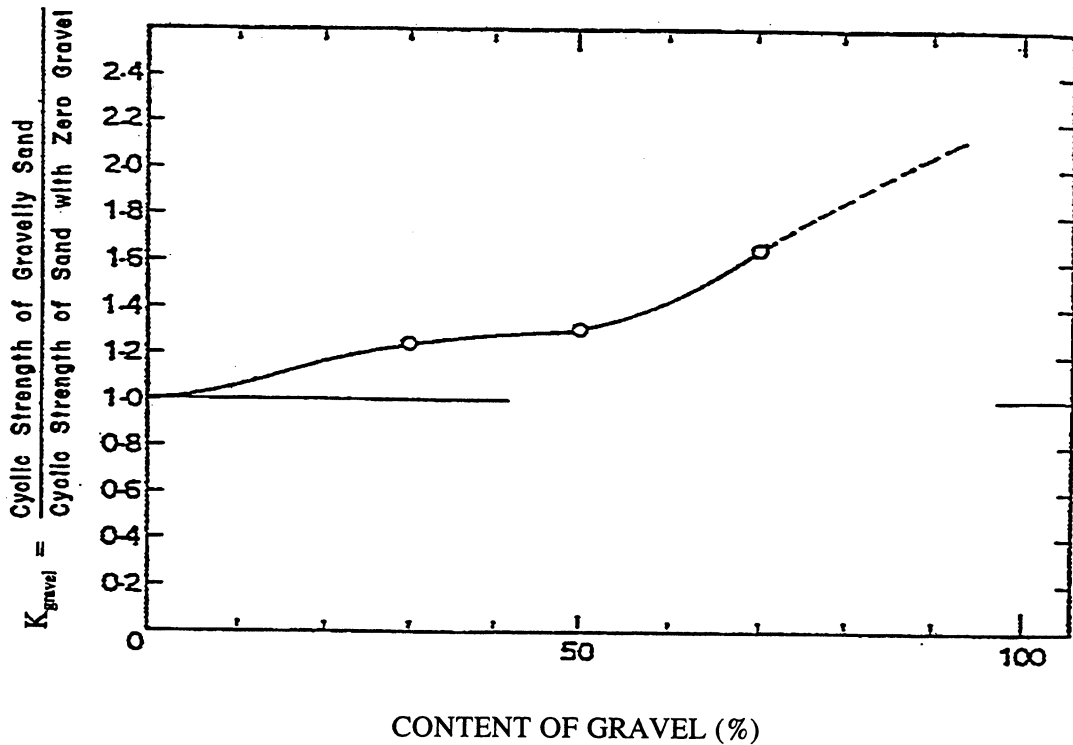


Figure 8-7: Effects of Gravel Content on Liquefaction Resistance of Gravelly Soils (Ishihara, 1985)

with Zero Gravel” cited in the figure should be obtained from the sand layers at the site in the vicinity of the gravelly soil deposit, provided that the sand layers (without gravel) and the gravelly soil layers were formed under the same geological conditions.

Step 9: Calculate the factor of safety against initial liquefaction, FS_L , as:

$$FS_L = \frac{CSR_L}{CSR_{EQ}} \quad (8-5)$$

There is no general agreement on the appropriate minimum factor of safety against liquefaction (NRC, 1985). There are cases where liquefaction-induced instability has occurred prior to complete liquefaction, i.e., with a factor of safety against initial liquefaction greater than 1.0. For regular highway bridge design, it is recommended that a minimum factor of safety of 1.1 against liquefaction be required.

It should be noted that the Simplified Procedure is aimed primarily at moderately strong ground motions ($0.2 \text{ g} < a_{\max} < 0.5 \text{ g}$). If the peak horizontal acceleration is larger than 0.5 g, more sophisticated, truly non-linear effective stress-based analytical approaches may be advisable. Computer programs for evaluation of liquefaction potential as a part of a site response analysis include the one-dimensional response analysis computer program DESRA-2 (Lee and Finn, 1978) and its derivative codes MARDES (Chang, *et al.*, 1991), D-MOD (Matasović, 1993), and SUMDES (Li, *et al.*, 1992) as well as two-dimensional codes such as DYNFLOW (Prevost, 1981), TARA-3 (Finn, *et al.*, 1986), LINOS (Bardet, 1992), DYSAC2 (Muraleetharan, *et al.*, 1991), and certain adaptations of FLAC (Cundall and Board, 1988) (e.g., Roth and Inel, 1993). These computer programs are briefly discussed in Chapter 6.

An example of a liquefaction analysis performed using the Simplified Procedure is presented in Part II of this document.

8.3.3 Variations on the Simplified Procedure

The principle variations on the simplified procedure used in practice include the use of CPT resistance and shear wave velocity, instead of the normalized SPT blow count to evaluate the critical stress ratio, causing liquefaction for a magnitude 7.5 earthquake, $CSR_{7.5}$. Figure 8-8 presents the relationship between corrected CPT tip resistance, q_{C1N} , and $CSR_{7.5}$, where q_{C1N} is evaluated from the tip resistance q_c as follows:

$$q_{C1N} = \left(\frac{P_a}{\sigma'_v} \right)^n \left(\frac{q_c}{P_a} \right) \quad (8-6)$$

where σ'_v is effective overburden pressure, P_a is atmospheric pressure (approximately 100 kPa) and n is an exponent that varies from 0.5 for clean sands, 0.7 for silty sands, and 0.8 for sandy silt.

It should be noted that Figure 8-8 is applicable for clean sands with fines less than 5%. To correct the normalized penetration resistance, q_{C1N} , of sands with fines greater than 5% to an equivalent clean sand value, $(q_{C1N})_{CS}$ the following relationship is used.

$$(q_{C1N})_{CS} = K_{CS} q_{C1N} \quad (8-7)$$

where K_{CS} varies from 1.0 for fines less than 5%, 1.4 for fines equal to 15%, to 3.35 for fines equal to 35%.

Simplified procedures using field measurements of small-strain shear wave velocity, V_s , to assess liquefaction resistance of granular soils have also been proposed. Figure 8-9 presents the relationship (Youd and Idriss, 1997) between $CSR_{7.5}$ and stress-corrected shear wave velocity, V_{S1} , where V_{S1} is calculated as:

$$V_{S1} = V_s \left(\frac{P_a}{\sigma'_v} \right)^{0.25} \quad (8-8)$$

The relationship shown in Figure 8-9 was developed based on data from many field sites (including the field performance data from the 1989 Loma Prieta earthquake) where liquefaction did or did not occur. Similar to the relationships developed using SPT and CPT data, the liquefaction resistance curves in Figure 8-9 are for magnitude 7.5 earthquakes and effective overburden pressures less than about 100 kPa. Appropriate correction factors as discussed in Section 8.3.2 should be applied to account for magnitudes other than 7.5 or effective overburden pressures greater than 100 kPa.

8.4 POST-LIQUEFACTION DEFORMATION AND STABILITY

For soil layers in which the factor of safety against initial liquefaction is unsatisfactory, a liquefaction impact analysis may demonstrate that the site will still perform adequately even if liquefaction occurs. Potential impacts of liquefaction include bearing capacity failure, loss of lateral support for piles, lateral spreading, and post-liquefaction settlement. These are all phenomena associated with large soil strains and

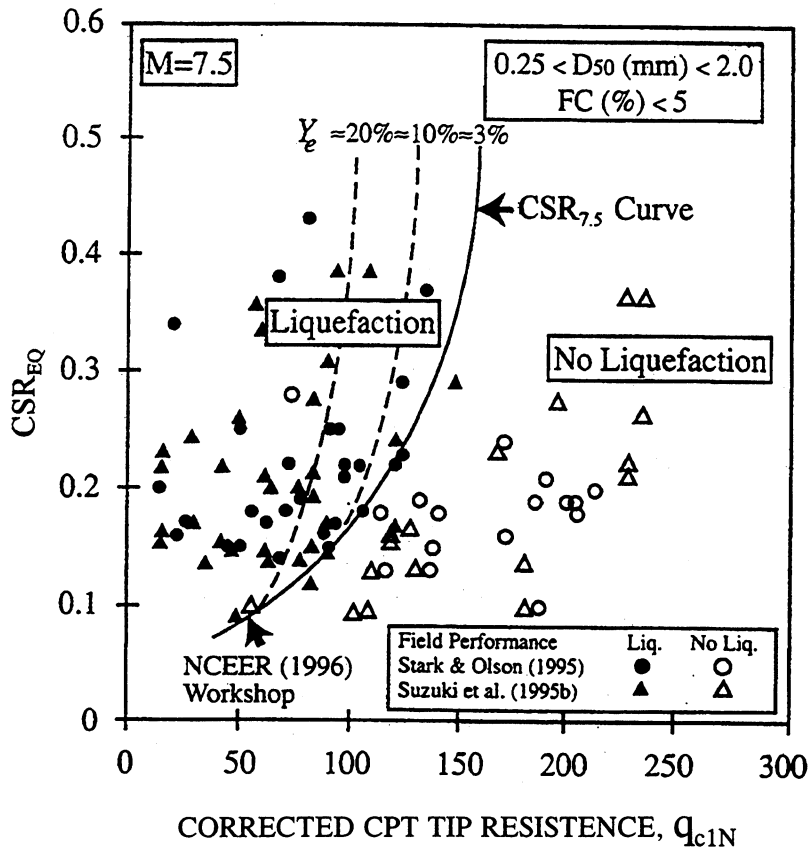


Figure 8-8: Relationship between Cyclic Stress Ratio Causing Liquefaction and CPT Tip Resistance, Q_{c1N} for Sands for $M = 7.5$ (Robertson and Wride, 1997)

ground deformations. Relatively dense soils which liquefy may subsequently harden or stabilize at small deformations and thus have minimal impact on overlying highway structures. Conversely, relatively loose soils that liquefy will tend to collapse resulting in a much greater potential for post-liquefaction deformation. Methods for assessing the impact of liquefaction generally are based upon evaluation of the strain or deformation potential of the liquefiable soil. A liquefaction impact analysis for highway-related projects may consist of the following steps:

Step 1: Calculate the magnitude and distribution of liquefaction-induced settlement by multiplying the post-liquefaction volumetric strain, ϵ_v , by the thickness of the liquefiable layer, H .

The post-liquefaction volumetric strain can be estimated from the chart presented in Figure 8-10 (Tokimatsu and Seed, 1987). An alternative chart has recently been proposed by Ishihara (1993). Note that both charts were developed for clean sands and tend to overestimate settlements of sandy silts and silts. Application of Ishihara's chart requires translation of normalized SPT blow count $(N_1)_{60}$ values determined in Chapter 5 to Japanese-standard N_j values ($N_j = 0.833 (N_1)_{60}$; after Ishihara, 1993). The magnitude of liquefaction-induced settlement should be calculated at each SPT or CPT sounding location to evaluate the potential variability in seismic settlement across the project site.

Step 2: Estimate the free-field liquefaction-induced lateral displacement, Δ_L . The empirical equation proposed by Hamada, *et al.* (1987) may be used to estimate Δ_L in meters:

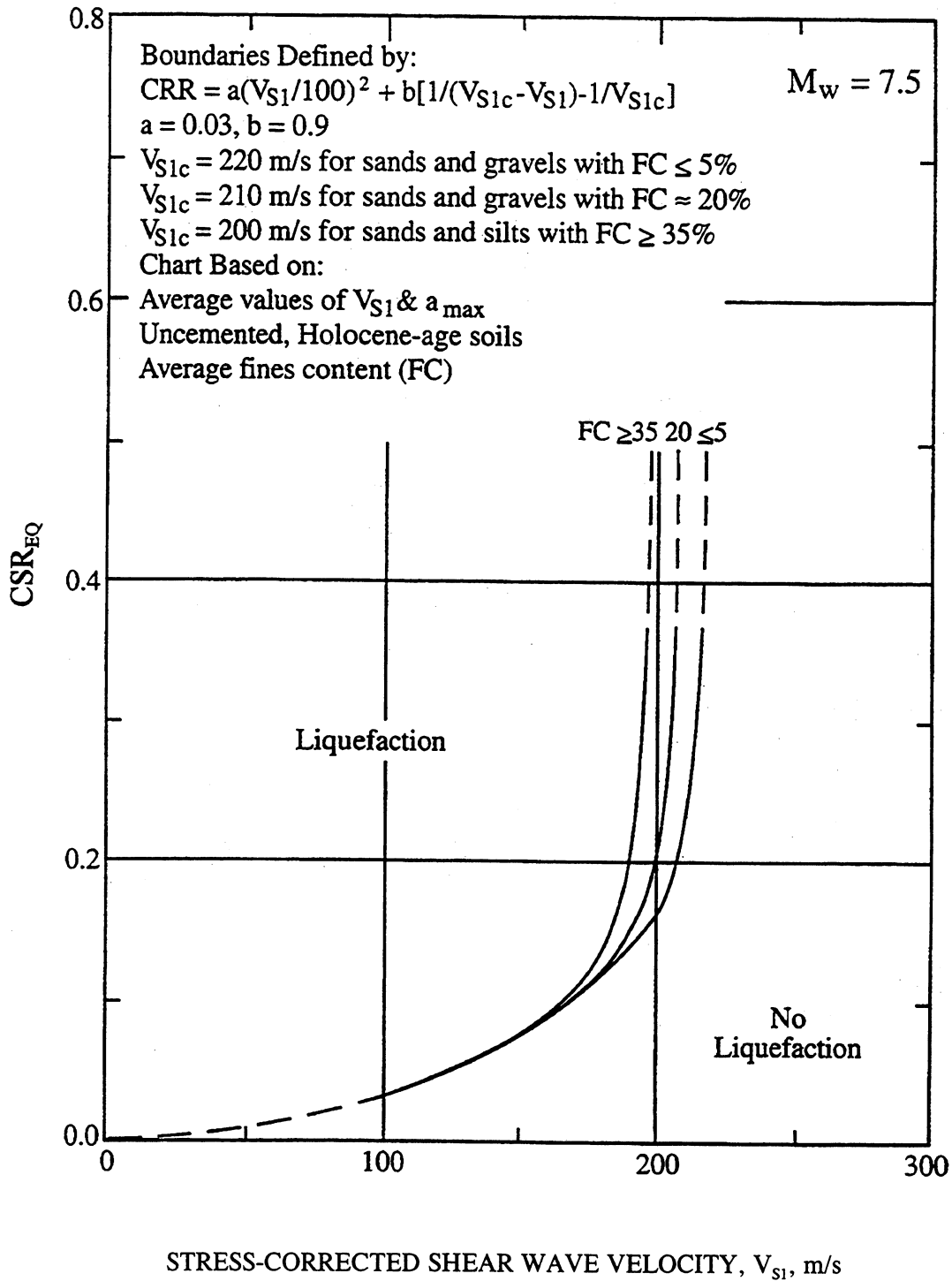


Figure 8-9: Relationship Between Cyclic Stress Ratio Causing Liquefaction and Shear Wave Velocity Values, V_{S1} , for Sands for $M = 7.5$ Earthquakes (Youd and Idriss, 1997)

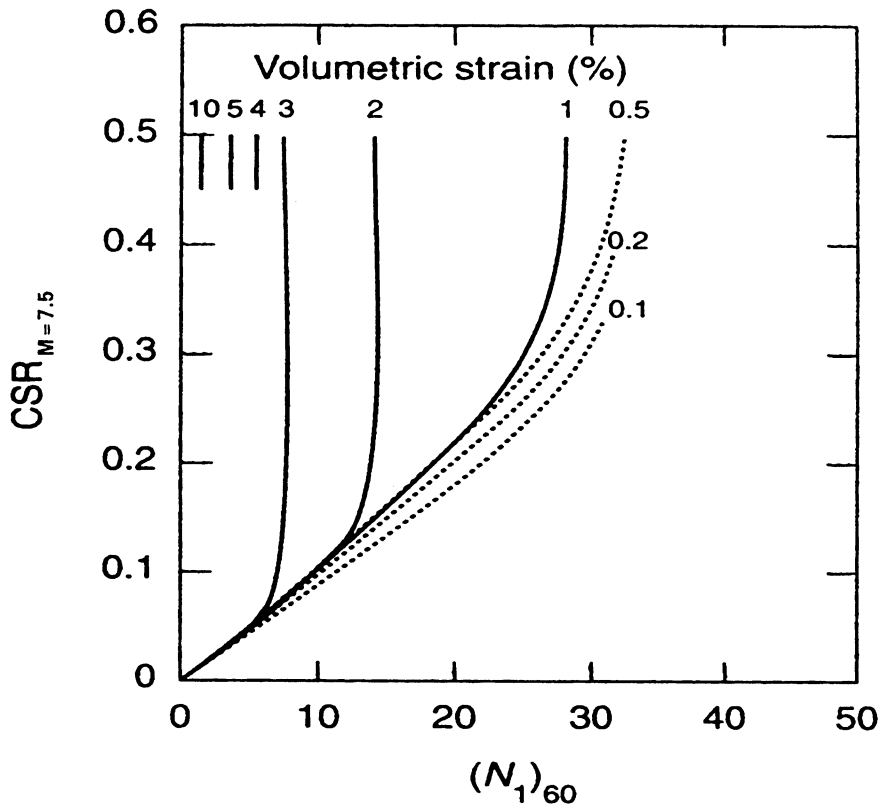


Figure 8-10: Curves for Estimation of Post-Liquefaction Volumetric Strain Using Spt Data and Cyclic Stress Ratio for M_w 7.5 Earthquakes. (Tokimatsu and Seed, 1987, reprinted by permission of ASCE).

$$\Delta_L = 0.75 (H)^{1/2} (S)^{1/3} \quad (8-9)$$

where H is the thickness of the liquefied layer in meters and S is the ground slope in percent.

The Hamada, *et al.* (1987) formula in Equation 8-9 is based primarily on Japanese data (for major earthquakes of magnitude 7.5 or greater) on observed liquefaction displacements of very loose sand deposits having a slope, S , less than 10 percent. Therefore, Equation 8-9 should be assumed to provide only a rough upper bound estimate of lateral displacement. Since Equation 8-9 does not reflect either the density, or $(N_1)_{60}$ value, of the liquefiable soil or the depth of the liquefiable layer, it likely provides a conservative estimate of lateral displacement for denser sands or for cases where the soil liquefies at depth. Estimates of lateral displacement obtained using Equation 8-9 may indicate excessive liquefaction-induced lateral displacements in areas of essentially flat ground conditions.

A more accurate empirical procedure for assessing lateral spreading was developed by Bartlett and Youd (1995). This procedure was developed from multiple linear regression analyses of U.S. and Japanese case histories. Two general types of lateral spreading are differentiated according to Bartlett and Youd's study: (1) lateral spread towards a free face, and (2) lateral spread down gentle ground slopes where a free face is absent. The procedure is summarized as follows:

- (1) If $(N_1)_{60}$ values are equal to or more than 15, the potential for lateral displacements would be small for earthquakes with magnitudes less than 8.0, and no additional

analyses are warranted.

- (2) If $(N_1)_{60}$ values are less than 15, then the evaluation of lateral displacement is performed using the following equations:

For free-face conditions:

$$\begin{aligned} \text{Log}\Delta_L = & -16.366 + 1.178M - 0.927\text{Log } R - 0.013R + 0.657\text{Log } W \\ & + 0.348\text{Log } H_{15} + 4.527\text{Log } (100 - F_{15}) - 0.922D50_{15} \end{aligned} \quad (8-10a)$$

For ground slope conditions:

$$\begin{aligned} \text{Log}\Delta_L = & -15.787 + 1.178M - 0.927\text{Log } R - 0.013R + 0.429\text{Log } S \\ & + 0.348\text{Log } H_{15} + 4.527\text{Log } (100 - F_{15}) - 0.922D50_{15} \end{aligned} \quad (8-10b)$$

Where:

- Δ_L = Estimated lateral ground displacement in meters
- H_{15} = Cumulative thickness of saturated granular layers with corrected blow counts, $(N_1)_{60}$, less than or equal to 15, in meters.
- $D50_{15}$ = Average mean grain size in granular layer included in H_{15} in mm.
- F_{15} = Average fines content for granular layers included in H_{15} in percent.
- M = Earthquake magnitude (moment magnitude).
- R = Horizontal distance from seismic energy source, in kilometers.
- S = Ground slope, in percent.
- W = Ratio of the height (H) of the free face to the distance (L) from the base of the free face to the point in question, in percent (i.e., $100H/L$).

Step 3: In areas of significant ground slope, or in situations when a deep failure surface may pass through the body of the facility or through underlying liquified layers, a flow slide can occur following liquefaction. The potential for flow sliding should be checked using a conventional limit equilibrium approach for slope stability analyses (discussed in Chapter 7) together with residual shear strengths in zones in which liquefaction may occur. Residual shear strengths can be estimated from the penetration resistance values of the soil using the chart proposed by Seed, *et al.* (1988) presented in Figure 5-15. Seed and Harder (1990) and Marcuson, *et al.* (1990) present further guidance for performing a post-liquefaction stability assessment using residual shear strengths.

If liquefaction-induced vertical and/or lateral deformations are large, the integrity of the highway facility may be compromised. The question the engineer must answer is "What magnitude of deformation is too large?" The magnitude of acceptable deformation should be established by the design engineer on a case-by-case basis. Calculated seismic deformations on the order of 0.15 to 0.30 m are generally deemed to be acceptable in current practice for highway embankments in California. For highway system components other than embankments, engineering judgement must be used in determining the allowable level of calculated seismic deformation. For example, components that are designed to be unyielding, such as bridge abutments restrained by batter piles, may have more restrictive deformation requirements than structures which can more easily accommodate foundation deformations. At the current time,

determination of allowable deformations remains a subject requiring considerable engineering judgement.

8.5 SEISMIC SETTLEMENT EVALUATION

Both unsaturated and saturated sands tend to settle and densify when subjected to earthquake shaking. If the sand is saturated and there is no possibility for drainage, so that constant volume conditions are maintained, the primary initial effect of the shaking is the generation of excess pore water pressures. Settlement then occurs as the excess pore pressures dissipate. In unsaturated sands, on the other hand, settlement may occur during the earthquake shaking under conditions of constant effective vertical stress (depending on the degree of saturation). In both cases (saturated and unsaturated soil), however, one result of strong ground shaking is settlement of the soil.

Liquefaction induced settlement of saturated sand is addressed as part of a post-liquefaction deformation and stability assessment as described in Section 8.4 of this Chapter. A procedure for evaluating the seismic settlement of unsaturated sand, following the general procedure presented in Tokimatsu and Seed (1987), is outlined below.

Seismic settlement analysis of unsaturated sand can be performed using the following steps:

Step 1: From borings and soundings, in situ testing and laboratory index tests, develop a detailed understanding of the project site subsurface conditions, including stratigraphy, layer geometry, material properties and their variability, and the areal extent of potential problem zones. Establish the zones to be analyzed and develop idealized, representative sections amenable to analysis. The subsurface data used to develop the representative sections should include normalized standardized SPT blow counts, $(N_1)_{60}$ (or results of some other test, e.g., the CPT from which $(N_1)_{60}$ can be inferred) and the unit weight of the soil.

Step 2: Evaluate the total vertical stress, σ_v , and the mean normal effective stress, σ'_m , at several layers within the deposit at the time of exploration and for design. The design values should include stresses resulting from highway facility construction. Outside of the highway facility footprint, the exploration and design values are generally the same.

Step 3: Evaluate the stress reduction factor, r_d , using one of the approaches presented in step 3 of Section 8.3 of this Chapter.

Step 4: Evaluate γ_{eff} ($G_{\text{eff}}/G_{\text{max}}$) using the Tokimatsu and Seed (1987) equation:

$$\gamma_{\text{eff}} (G_{\text{eff}} / G_{\text{max}}) = (0.65 \cdot a_{\text{max}} \cdot \sigma_v \cdot r_d) / (g \cdot G_{\text{max}}) \quad (8-11)$$

where γ_{eff} ($G_{\text{eff}}/G_{\text{max}}$) is a *hypothetical effective shear stress factor*, a_{max} is the peak ground surface acceleration, g is the acceleration of gravity, and G_{max} is the shear modulus of the soil at small strain. Note that $G_{\text{max}} = \rho \cdot V_s^2$, where V_s is the shear wave velocity and ρ is the mass density of the soil. Alternatively, G_{max} (in kPa) can be evaluated from the correlation given below (Seed and Idriss, 1970):

$$G_{\text{max}} = 4,400[(N_1)_{60}]^{1/3} (\sigma'_m)^{1/2} \quad (8-12)$$

where $(N_1)_{60}$ is the normalized standardized SPT blow count defined before and σ'_m is mean normal effective stress in kPa. For unsaturated sands, σ'_m can be estimated using Equation 5-12.

However, for most practical purposes, the approximation $\sigma'_m \approx 0.65 \sigma'_v$ will suffice.

- Step 5: Evaluate γ_{eff} as a function of $\gamma_{\text{eff}} (G_{\text{eff}}/G_{\text{max}})$ and σ'_m using the chart reproduced in Figure 8-11.
- Step 6: Assuming that $\gamma_{\text{eff}} \approx \gamma_c$, where γ_c is the cyclic shear strain, evaluate the volumetric strain due to compaction, ϵ_c , for an earthquake of magnitude 7.5 (15 cycles) using the chart reproduced in Figure 8-12.
- Step 7: Correct for earthquake (moment) magnitude other than M_w 7.5 using the correction factors reproduced in Table 8-2.
- Step 8: Multiply the volumetric strain due to compaction for each layer by two to correct for the multidirectional shaking effect, as recommended by Tokimatsu and Seed (1987), to get the representative volumetric strain for each layer.
- Step 9: Calculate seismic settlements of each layer by multiplying the layer thickness by the representative volumetric strain evaluated in Step 8. Sum up the layer settlements to obtain the total seismic settlement for the analyzed profile.

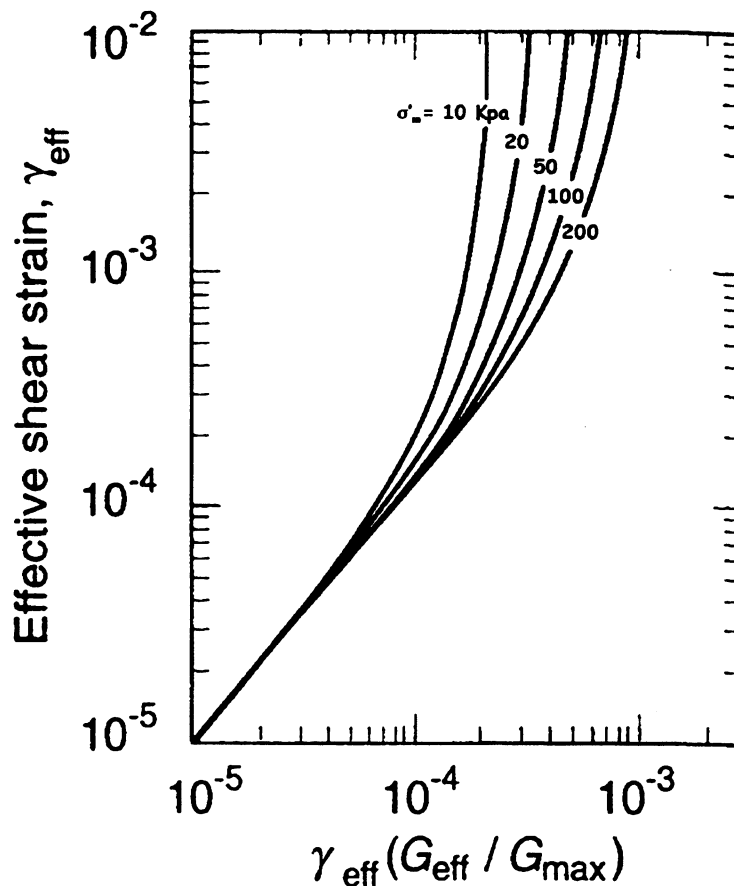


Figure 8-11: Plot for Determination of Earthquake-Induced Shear Strain in Sand Deposits. (Tokimatsu and Seed, 1987, reprinted by permission of ASCE)

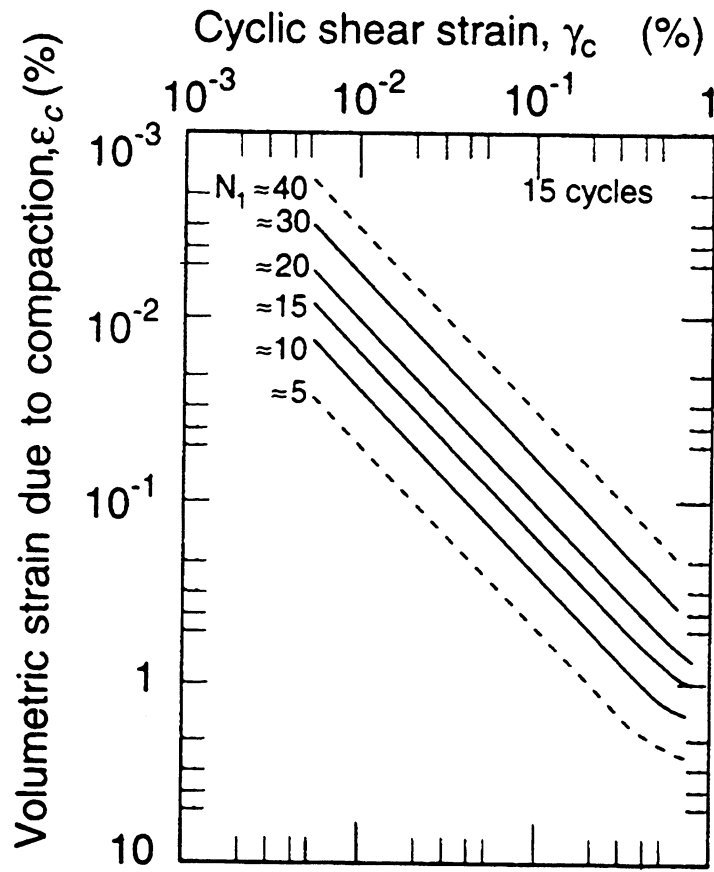


Figure 8-12: Relationship Between Volumetric Strain, Cyclic Shear Strain, and Penetration Resistance for Unsaturated Sands. (Tokimatsu and Seed, 1987, reprinted by permission of ASCE)

TABLE 8-2
INFLUENCE OF EARTHQUAKE MAGNITUDE
ON VOLUMETRIC STRAIN RATIO FOR DRY SANDS
 (After Tokimatsu and Seed, 1987, Reprinted by Permission of ASCE)

Earthquake Magnitude	Number of Representative Cycles at $0.65 \tau_{max}$	Volumetric Strain Ratio $\epsilon_{c,N}/\epsilon_{c,N=15}$
8.5	26	1.25
7.5	15	1.0
6.75	10	0.85
6	5	0.6
5.25	2-3	0.4

Considerable judgement is required when evaluating the performance of a highway facility based on an estimate of seismic settlement. The magnitude of calculated seismic settlement should be considered primarily as an indication of whether settlements are relatively small (several centimeters) or relatively large (several meters). A more precise evaluation of seismic settlement is not within the capabilities of conventional engineering analyses using the simplified methods presented herein.

8.6 LIQUEFACTION MITIGATION

If the seismic impact analyses presented in Sections 8.4 and 8.5 yield unacceptable deformations, consideration may be given to performing a more sophisticated liquefaction potential assessment and to evaluation of liquefaction potential mitigation measures. Generally, the engineer has the following options: (1) proceed with a more advanced analysis technique; (2) design the facility to resist the anticipated deformations; (3) remediate the site to reduce the anticipated deformations to acceptable levels; or (4) choose an alternative site. If a more advanced analysis still indicates unacceptable impacts from liquefaction, the engineer must still consider options (2) through (4). These options may require additional subsurface investigation, advanced laboratory testing, more sophisticated numerical modeling, and, in rare cases, physical modeling. Discussion of these techniques is beyond the scope of this document.

Options that may be considered when designing to resist anticipated deformation include the use of ductile pile foundations, reinforced earth, structural walls, or buttress fills keyed into non-liquefiable strata to resist the effects of lateral spreading. These techniques are described in detail elsewhere (e.g., Kramer and Holtz, 1991).

A variety of techniques exist to remediate potentially liquefiable soils and mitigate the liquefaction hazard. Table 8-3 presents a summary of methods for improvement of liquefiable soil foundation conditions (NRC, 1985). The cost of foundation improvement can vary over an order of magnitude, depending on site conditions (e.g., adjacent sensitive structures) and the nature and geometry of the liquefiable soils. Remediation costs can vary from as low as several thousand dollars per acre for dynamic compaction of shallow layers of clean sands in open areas to upwards of \$100,000 per acre for deep layers of silty soils adjacent to sensitive structures. Liquefaction remediation measures must be evaluated on a case-by-case basis to determine their economic viability.

The results of a number of post-earthquake settlement measurements made on Port Island and Rokko Island following the 1995 Kobe Earthquake in relation to site treatment methods are presented in Figure 8-13 (Yasuda, et al, 1995). The soil profile on these islands is typically 12 to 20 m of loose, hydraulically filled, decomposed granite sand underlain by several meters of soft, compressible alluvial clay. It should be noted that sand drains and preloading were used for the purpose of precompressing the soft clay for reducing future long term settlements under static loads. The results shown in Figure 8-13 suggest that sand drains and preloading, although have some beneficial effects on the liquefaction resistance, are not effective methods in preventing liquefaction from occurring. To mitigate liquefaction risk of loose, granular soils, proper methods of ground treatment have to be applied.

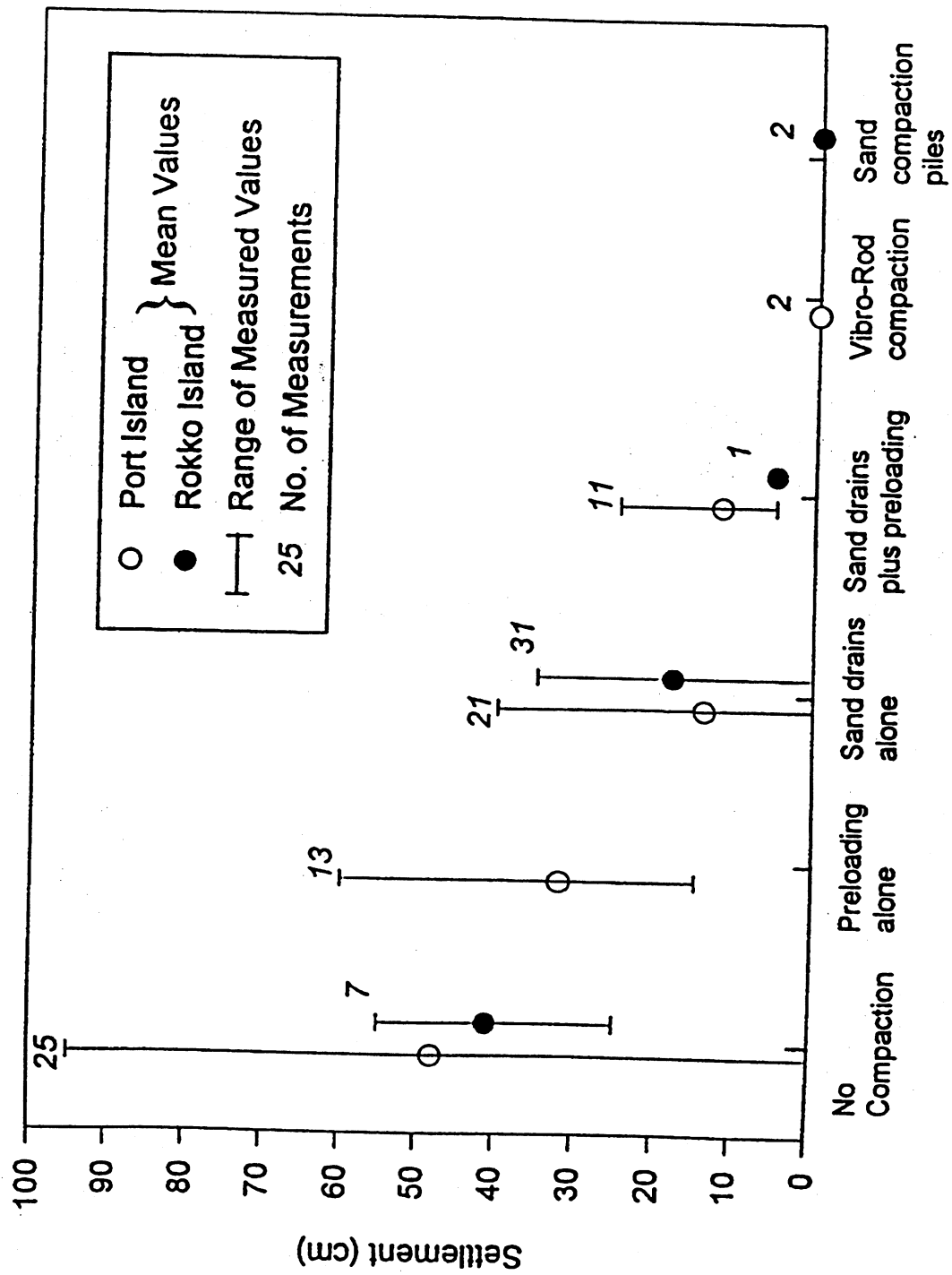


Figure 8-13: Post-Earthquake Settlements at Two Port Sites due to the 1995 Kobe Earthquake (Yasuda, et. al, 1995).

TABLE 8-3 IMPROVEMENT TECHNIQUES FOR LIQUEFIABLE SOIL FOUNDATION CONDITIONS (AFTER NRC, 1985)

Method	Principle	Most Suitable Soil Conditions/Types	Maximum Effective Treatment Depth	Economical Size of Treated Area	Ideal Properties of Treated Material*	Applications**	Case†	Relative Costs
In-Situ Deep Compaction								
(1) Blasting	Shock waves and vibrations cause limited liquefaction, displacement, remolding and settlement to higher density.	Saturated, clean sands; partly saturated sands and silts after flooding.	> 40 m Solyman (1984)	Any Size	Can obtain relative densities of 70-80%; may get variable density; time-dependent strength gain.	Induce liquefaction in controlled and limited stages and increase relative density to potentially non-liquefiable range.	2 3	Low
(2) Vibratory Probe (a) Terraprobe (b) Vibro-Rods (c) Vibro-Wing	Densification by vibration; liquefaction-induced settlement and settlement in dry soil under overburden to produce a higher density.	Saturated or dry clean sand; sand.	20 m routinely (ineffective above 3-4 m depth) > 30 m sometimes Mitchell (1981) Vibro-Wing-40 m Broms and Hansson (1984)	> 1,000 m ²	Can obtain relative densities of 80% or more. Ineffective in some sands.	Induce liquefaction in controlled and limited stages and increase relative density to potentially non-liquefiable range. Has been shown ineffective in preventing liquefaction.	2 3	Moderate
(3) Vibro-Compaction (a) Vibroflot (b) Vibro-Composer System (c) Soil Vibratory stabilizing method	Densification by vibration and compaction of backfill material of sand or gravel.	Cohesionless soils with less than 20% fines.	> 30 m Solyman et al. (1984)	> 1,000 m ²	Can obtain high relative densities (over 85%), good uniformity.	Induce liquefaction in controlled and limited stages and increase relative densities to nonliquefiable condition. Is used extensively to prevent liquefaction. The dense column of backfill provides (a) vertical support, (b) drains to relieve pore water pressure and (c) shear resistance in horizontal and inclined directions. Used to stabilize slopes and strengthen potential failure surfaces or slip circles.	1 2 Δ [†]	Low to moderate
(4) Compaction Soils	Densification by displacement of pile volume and by vibration during driving, increase in lateral effective earth pressure.	Loose sandy soils; partly saturated clayey soils; loess.	> 20 m Nataraja and Cook (1983)	> 1,000 m ²	Can obtain high relative densities, good uniformity. Relative densities of more than 80%.	Useful in soils with fines. Increases relative densities to nonliquefiable range. Is used to prevent liquefaction. Provides shear resistance in horizontal and inclined directions. Useful to stabilize slopes and strengthen potential failure surfaces or slip circles.	1 2 3	Moderate to High
(5) Heavy Tamping (dynamic compaction)	Repeated application of high-intensity impacts at surface.	Cohesionless soils best, other types can also be improved.	30 m (possibly deeper) Ménard and Broise (1975)	> 3,300 m ²	Can obtain high relative densities, reasonable uniformity. Relative densities of 80% or more.	Suitable for some soils with fines; usable above and below water. In cohesionless soils, induces liquefaction in controlled and limited stages and increases relative density to potentially nonliquefiable range. Is used to prevent liquefaction.	2 3	Low

* SP, SW, or SM soils which have average relative density equal to or greater than 85 percent and the minimum relative density not less than 80 percent are in general not susceptible to liquefaction (TM 5-818-1). D'Appolonia (1970) stated that for soil within the zone of influence and confinement of the structure foundation, the relative density should not be less than 70 percent. Therefore, a criterion may be used that relative density increase into the 70-90 percent range is in general considered to prevent liquefaction. These properties of treated materials and applications occur only under ideal conditions of soil, moisture, and method application. The methods and properties achieved are not applicable and will not occur in all soils.

** Applications and results of the improvement methods are dependent on: (a) soil profiles, types, and conditions, (b) site conditions, (c) earthquake loading, (d) structure type and condition, and (e) material and equipment availability. Combinations of the methods will most likely provide the best and most stable solution.

† Site conditions have been classified into three cases; Case 1 is for beneath structures, Case 2 is for the not-under-water free field adjacent to a structure, and Case 3 is for the under-water free field adjacent to a structure.

Δ means the method has potential use for Case 3 with special techniques required which would increase the cost.

TABLE 8-3 IMPROVEMENT TECHNIQUES FOR LIQUEFIABLE SOIL FOUNDATION CONDITIONS (AFTER NRC, 1985)

Method	Principle	Most Suitable Soil Conditions/Types	Maximum Effective Treatment Depth	Economical Size of Treated Area	Ideal Properties of Treated Material*	Applications**	Case ¹	Relative Costs
In-Situ Deep Compaction								
(6) Displacement/Compaction Grout	Highly viscous grout acts as radical hydraulic jack when pumped in under high pressure.	All soils.	Unlimited	Small	Grout bulbs within compressed soil matrix. Soil mass as a whole is strengthened.	Increase in soil relative density and horizontal effective stress. Reduce liquefaction potential. Stabilize the ground against movement.	1 2 3	Low to Moderate
Compression								
(7) Surcharge/Buttress	The weight of a surcharge/buttress increases the liquefaction resistance by increasing the effective confining pressures in the foundation.	Can be placed on any soil surface.	—	> 1,000 m ²	Increase strength and reduce compressibility.	Increase the effective confining pressure in a liquefiable layer. Can be used in conjunction with vertical and horizontal drains to relieve pore pressure. Reduce liquefaction potential. Useful to prevent movements of a structure and for slope stability.	2 3	Moderate if vertical drains used.
Pore-Water Pressure Relief								
(8) Drains (a) Gravel (b) Sand (c) Wick (d) Wells (for permanent dewatering)	Relief of excess pore-water pressure to prevent liquefaction. (Wick drains have comparable permeability to sand drains). Primarily gravel drains; sand/wick drains may supplement gravel drain or relieve existing excess pore water pressure. Permanent dewatering with pumps.	Sand, silt, clay.	Gravel and Sand > 30 m Depth limited by vibratory equipment Wick > 45 m Morrison (1982)	> 1,500 m ² Any size for wick.	Pore-water pressure relief will prevent liquefaction.	Prevent liquefaction by gravel drains. Sand and gravel drains are installed vertically; however, wick drains can be installed at any angle. Dewatering will prevent liquefaction but not seismically-induced settlements.	Gravel and Sand 2 3 Δ ¹ Wick 1 2 3	Dewatering very expensive.
(9) Particulate Grouting	Penetration grouting - fill soil pores with soil, cement, and/or clay.	Medium to coarse sand and gravel.	Unlimited	Small	Impervious, high strength with cement grout. Voids filled so they cannot collapse under cyclic loading.	Eliminate liquefaction danger. Slope stabilization. Could potentially be used to confine an area of liquefiable soil so that liquefied soil could not flow out of the area.	1 2 3	Lowest of Grout Methods

* SP, SW, or SM soils which have average relative density equal to or greater than 85 percent and the minimum relative density not less than 80 percent are in general not susceptible to liquefaction (TM 5-818-1). D'Appolonia (1970) stated that for soil within the zone of influence and confinement of the structure foundation, the relative density should not be less than 70 percent. Therefore, a criterion may be used that relative density increase into the 70-90 percent range is in general considered to prevent liquefaction. These properties of treated materials and applications occur only under ideal conditions of soil, moisture, and method application. The methods and properties achieved are not applicable and will not occur in all soils.

** Applications and results of the improvement methods are dependent on: (a) soil profiles, types, and conditions, (b) site conditions, (c) earthquake loading, (d) structure type and condition, and (e) material and equipment availability. Combinations of the methods will most likely provide the best and most stable solution.

¹ Site conditions have been classified into three cases; Case 1 is for beneath structures, Case 2 is for the not-under-water free field adjacent to a structure, and Case 3 is for the under-water free field adjacent to a structure.

² Δ means the method has potential use for Case 3 with special techniques required which would increase the cost.

TABLE 8-3 IMPROVEMENT TECHNIQUES FOR LIQUEFIABLE SOIL FOUNDATION CONDITIONS (AFTER NRC, 1985)

Method	Principle	Most Suitable Soil Conditions/Types	Maximum Effective Treatment Depth	Economical Size of Treated Area	Ideal Properties of Treated Material*	Applications**	Case [†]	Relative Costs
(10) Chemical Grouting	Solutions of two or more chemicals react in soil pores to form a gel or a solid precipitate.	Medium silts and coarser.	Unlimited	Small	Impervious, low to high strength. Voids filled so they cannot collapse under cyclic loading.	Eliminate liquefaction danger. Slope stabilization. Could potentially be used to confine an area of liquefiable soil so that liquefied soil could not flow out of the area. Good water shutoff.	1 2 3	High
(11) Pressure-Injected Lime	Penetration grouting - fill soil pores with lime.	Medium to coarse sand and gravel.	Unlimited	Small	Impervious to some degree. No significant strength increase. Collapse of voids under cyclic loading reduced.	Reduce liquefaction potential.	1 2 3	Low
Pore-Water Pressure Relief								
(12) Electrokinetic Injection	Stabilizing chemicals move into and fill soil pores by electro-osmosis or colloids into pores by electrophoresis.	Saturated sands, silts, silty clays.	Unknown	Small	Increased strength, reduced compressibility, voids filled so they cannot collapse under cyclic loading.	Reduce liquefaction potential.	1 2 3	Expensive
(13) Jet Grouting	High-speed jets at depth excavate, inject, and mix a stabilizer with soil to form columns or panels.	Sands, silts, clays.	Unknown	Small	Solidified columns and walls.	Slope stabilization by providing shear resistance in horizontal and inclined directions which strengthens potential failure surfaces or slip circles. A wall could be used to confine an area of liquefiable soil so that liquefied soil could not flow out of the area.	1 2 3	High
Admixture Stabilization								
(14) Mix-in-Place Piles and Walls	Lime, cement, or asphalt introduced through rotating auger or special in-place mixer.	Sands, silts, clays, all soft or loose inorganic soils.	>20 m (60 m obtained in Japan) Mitchell (1981)	Small	Solidified soil piles or walls of relatively high strength.	Slope stabilization by providing shear resistance in horizontal and inclined directions which strengthens potential failure surfaces or slip circles. A wall could be used to confine an area of liquefiable soil so that liquefied soil could not flow out of the area.	1 2 3	High

* SP, SW, or SM soils which have average relative density equal to or greater than 85 percent and the minimum relative density not less than 80 percent are in general not susceptible to liquefaction (TM 5-818-1). D'Appolonia (1970) stated that for soil within the zone of influence and confinement of the structure foundation, the relative density should not be less than 70 percent. Therefore, a criterion may be used that relative density increase into the 70-90 percent range is in general considered to prevent liquefaction. These properties of treated materials and applications occur only under ideal conditions of soil, moisture, and method application. The methods and properties achieved are not applicable and will not occur in all soils.

** Applications and results of the improvement methods are dependent on: (a) soil profiles, types, and conditions, (b) site conditions, (c) earthquake loading, (d) structure type and condition, and (e) material and equipment availability. Combinations of the methods will most likely provide the best and most stable solution.

† Site conditions have been classified into three cases; Case 1 is for beneath structures, Case 2 is for the not-under-water free field adjacent to a structure, and Case 3 is for the under-water free field adjacent to a structure.

TABLE 8-3 IMPROVEMENT TECHNIQUES FOR LIQUEFIABLE SOIL FOUNDATION CONDITIONS (AFTER NRC, 1985)

Method	Principle	Most Suitable Soil Conditions/Types	Maximum Effective Treatment Depth	Economical Size of Treated Area	Ideal Properties of Treated Material	Applications**	Case [†]	Relative Costs
Thermal Stabilization								
(15) In-Situ Vitricification	Melts soil in place to create an obsidian-like vitreous material.	All soils and rock.	> 30 m Verbal from Battelle Laboratories	Unknown	Solidified soil piles or walls of high strength. Impervious; more durable than granite or marble; compressive strength, 9-11 ksi; splitting tensile strength, 1-2 ksi	Slope stabilization by providing shear resistance in horizontal and inclined directions which strengths potential failure surfaces or slip circles. A wall could be used to confine an area of liquefiable soil so that liquefied soil could not flow out of the area.	1 2 3	Moderate
Soil Reinforcement								
(16) Vitro-Replacement Stone and Sand Columns (a) Grouted (b) Not Grouted	Hole jetted into fine-grained soil and backfilled with densely compacted gravel or sand hole formed in cohesionless soils by vibro techniques and compaction of backfilled gravel or sand. For grouted columns, voids filled with a grout.	Sands, silts, clays.	> 30 m Limited by vibratory equipment.	> 1,300 m ² Fine-grained soils > 1,000 m ²	Increased vertical and horizontal load carrying capacity. Density increase in cohesionless soils. Shorter drainage paths.	Provides: (a) vertical support, (b) drains to relieve pore water pressure, and (c) shear resistance in horizontal and inclined direction. used to stabilize slopes and strengthen potential failure surfaces or slip circles. For grouted columns, no drainage provided but increased shear resistance. In cohesionless soil, density increase reduces liquefaction potential.	1 2 Δ [‡]	Moderate
(17) Root Piles, Soil Nailing	Small-diameter inclusions used to carry tension, shear, compression.	All soils.	Unknown.	Unknown	Reinforced zone of soil behaves as a coherent mass.	Slope stability by providing shear resistance in horizontal and inclined directions to strengthen potential failure surfaces or slip circles. Both vertical and angled placement of the piles and nails.	1 2 3	Moderate to High

* SP, SW, or SM soils which have average relative density equal to or greater than 85 percent and the minimum relative density not less than 80 percent are in general not susceptible to liquefaction (TM 5-818-1). D'Appolonia (1970) stated that for soil within the zone of influence and confinement of the structure foundation, the relative density should not be less than 70 percent. Therefore, a criterion may be used that relative density increase into the 70-90 percent range is in general considered to prevent liquefaction. These properties of treated materials and applications occur only under ideal conditions of soil, moisture, and method application. The methods and properties achieved are not applicable and will not occur in all soils.

** Applications and results of the improvement methods are dependent on: (a) soil profiles, types, and conditions, (b) site conditions, (c) earthquake loading, (d) structure type and condition, and (e) material and equipment availability. Combinations of the methods will most likely provide the best and most stable solution.

† Site conditions have been classified into three cases, Case 1 is for beneath structures, Case 2 is for the not-under-water free field adjacent to a structure, and Case 3 is for the under-water free field adjacent to a structure.

‡ Δ means the method has potential use for Case 3 with special techniques required which would increase the cost.